Surface Construction and Mechanisms of Adhesion in Tokay Gecko Feet and Characterization of a Bio-Inspired Reversible Adhesive Tape

Honors Undergraduate Thesis Submitted to:

The College of Engineering Honors Committee

College of Engineering

122 Hitchcock Hall

The Ohio State University

By:

Robert A. Sayer

Department of Mechanical Engineering

Spring 2006

Approved by:

Professor Bharat Bhushan, Advisor

Department of Mechanical Engineering

Acknowledgements

I would like to thank Professor Bharat Bhushan for providing me the opportunity to work in the NLIM and the many hours that he spent helping revise the literature review. I also greatly appreciate the help that I received from Dr. Zhenhua Tao with the AFM and from Yong Chae Jung with the optical profiler and the contact angle measurements and Dr. Manuel Palacio for obtaining the SEM images. Without the aforementioned people, this project would not have been possible.

Abstract

Several creatures including insects, spiders, and lizards, have developed a unique clinging ability that utilizes dry adhesion. Geckos, in particular, have developed the most complex adhesive structures capable of smart adhesion—the ability to cling on different smooth and rough surfaces and detach at will. These animals make use of on the order of a million microscale hairs (setae) (about 14000/mm^2) that branch off into hundreds of nanoscale spatulae. This hierarchical surface construction gives the gecko the adaptability to create a large real area of contact with surfaces. van der Waals forces are the primary mechanism utilized to adhere to surfaces and capillary forces are a secondary effect that can further increase adhesive force. Although a gecko is capable of producing on the order of 20 N of adhesive force, it retains the ability to remove its feet from an attachment surface at will. A man-made fibrillar structure capable of replicating gecko adhesion has the potential for use in dry, superadhesive tapes that would be of use in a wide range of applications. These adhesives could be created using micro/nanofabrication techniques or self-assembly.

A fibrillar polyvinylsiloxane (PVS) sample consisting of an array pillars (about 230/mm^2) approximately 50 μm in diameter, 70 μm in height and 60 μm center-to-center was compared to an unstructured sample. Structured roughness was found to be more important than random roughness in adhesion. The added roughness of the structured sample increased the hydrophobicity of the surface.

Contents

List of Figures

List of Tables

Chapter 1

Introduction

The remarkable adhesive ability of geckos was first noted by Aristotle (Aristotle/Thompson, 1918, Book IX, Part 9). Even though the adhesive ability of geckos has been known for several millennia, little was understood about this phenomenon until the late nineteenth century when microscopic hairs covering the toes of the gecko were first noted. The development of electron microscopy in the 1950s enabled scientists to view a complex hierarchical morphology that covers the skin on the gecko's toes. The skin is comprised of a complex fibrillar structure of lamellae (scansors), setae, branches, and spatulae (Ruibal and Ernst, 1965).

As shown in Figure 1 (Gao et al., 2005; Autumn, 2006), the gecko consists of an intricate hierarchy of structures beginning with lamellae, soft ridges that are 1-2 mm in length (Ruibal and Ernst, 1965) that are located on the attachment pads (toes) that compress easily so that contact can be made with rough bumpy surfaces. Tiny curved hairs known as setae extend from the lamellae (about 14,000 setae/mm^2) (Schleich and Kästle, 1986; Autumn and Peattie, 2002). These setae are typically 30-130 μm in length and 5-10 μm in diameter (Ruibal and Ernst, 1965; Hiller, 1968; Russell, 1975; Williams and Peterson, 1982). At the end of each seta, 100 to 1000 spatulae (Ruibal and Ernst, 1965; Hiller, 1968) with a diameter of 0.1-0.2 μm (Ruibal and Ernst, 1965) branch out

and form the points of contact with the surface. This hierarchical structure enables the gecko to create a real area of contact with a mating surface.

Over the past century and a half, several scientific studies have been conducted to determine the mechanisms of adhesion utilized by the gecko attachment system (Wagler, 1830; Simmermacher, 1884; Schmidt, 1904; Dellit, 1934; Ruibal and Ernst, 1965; Hiller, 1968; Gennaro, 1969; Stork, 1980; Autumn et al., 2000, 2002; Bergmann and Irschick, 2005; Huber et al., 2005b). It was first believed that geckos adhered to surfaces by secreting sticky fluids from glands in their toes. Other proposed mechanisms include suction (Simmermacher, 1884), electrostatic attractive charges (Schmidt, 1904), increased frictional force due to an increased real area of contact (Hora, 1923), and microinterlocking, where the spatulae act as hooks to grip to a surface much like microscale Velcro (Dellit, 1934). All of these mechanisms have been unsupported during testing.

Hiller (1968) proposed that van der Waals and capillary forces could be the sole source of adhesion. Recent literature supports van der Waals forces as the primary adhesive force (Autumn et al., 2000, 2002; Bergmann and Irschick, 2005, Huber et al., 2005a) and capillary forces as a secondary adhesive mechanism (Huber et al., 2005b).

van der Waals bonds are secondary bonds that are weak in comparison to other physical bonds. However, the van der Waals force between two surfaces is inversely proportional to the cube of the spacing between the two surfaces. As a result, if the spacing is on the order of atomic spacing (~0.3 nm) the van der Waals forces can be very large. Since gecko feet are comprised of a hierarchical structure that terminates in

elements on the nanoscale, a large area of the gecko skin is able to come into close proximity with random rough surfaces leading to large van der Waals forces.

Capillary forces arise when water vapor will condense to liquid on the surface of bulk materials due to the natural humidity present in the air. During contact this will cause the formation of adhesive bridges (menisci) due to the proximity of the two surfaces and the affinity of the surfaces. This effect can further increase the adhesive force of a gecko.

There is great interest among the scientific community to further study the characteristics of gecko feet in hope that this information could be applied to the production of micro/nanosurfaces capable of recreating the adhesive forces generated by these lizards. Common man-made adhesives such as tape or glue involve the use of wet adhesives that permanently attach two surfaces. However, replication of the characteristics of gecko feet would enable the development of a super adhesive polymer tape capable of clean, dry adhesion (e.g. Geim et al., 2003; Sitti, 2003; Sitti and Fearing, 2003a, 2003b; Northen and Turner, 2005a, 2005b; Yurdumakan et al., 2005). These reusable adhesives have potential for use in everyday objects such as tape, fasteners, and toys (e.g. Full et al., 2004) and in high technology such as microelectric and space applications (e.g. Northen and Turner, 2005a; Yurdumakan et al., 2005). Replication of the dynamic climbing and peeling ability of geckos could find use in the treads of wall-climbing robots (Sitti and Fearing, 2003b; Menon et al., 2004). Further characterization of these bio-inspired surfaces, including surface roughness and contact angle, are important if one is to design a reusable superadhesive.

A structured, bio-inspired polymer surface that exhibits high adhesive force was obtained for the study. The adhesive strength, friction force and surface characteristics of the sample were measured and compared to an unstructured surface.

Chapter 2

Gecko Feet: Natural Attachment Systems for Smart Adhesion

Almost 2500 years ago, the ability of the gecko to "run up and down a tree in any way, even with the head downwards" was observed by Aristotle (Aristotle/Thompson, 1918, Book IX, Part 9). This phenomenon is not limited to geckos, but occurs in several animals and insects as well. This universal attachment ability will be referred to as smart adhesion (Bhushan et al., 2006). Many insects (i.e. flies and beetles) and spiders have been the subject of investigation. Geckos, however, have been the most widely studied due to the fact that they exhibit the most versatile and effective adhesive known in nature. As a result, the vast majority of this chapter will be concerned with gecko feet.

Although there are nearly 700 species of geckos, the Tokay gecko (*Gekko gecko*) has been the main focus of scientific research (Hiller, 1968; Irschick et al., 1996). The Tokay gecko is the second largest gecko species, attaining lengths of approximately 0.3-0.4 m and 0.2-0.3 m for males and females, respectively. They have a distinctive blue or gray body with orange or red spots and can weigh up to 300 g (Tinkle, 1992). These geckos have been the most widely investigated species of gecko due to the availability and size of these creatures.

Even though the adhesive ability of geckos has been known since the time of Aristotle, little was understood about this phenomenon until the late nineteenth century when microscopic hairs covering the toes of the gecko were first noted. The development of electron microscopy in the 1950s enabled scientists to view a complex hierarchical morphology that covers the skin on the gecko's toes. Over the past century and a half, scientific studies have been conducted to determine the factors that allow the gecko to adhere and detach from surfaces at will, including surface structure (Ruibal and Ernst, 1965; Russell, 1975, 1986; Williams and Peterson, 1982; Schleich and Kästle, 1986; Irschick et al., 1996; Autumn and Peattie, 2002; Arzt et al, 2003;); the mechanisms of adhesion (Wagler, 1830; Simmermacher, 1884; Schmidt, 1904; Dellit, 1934; Ruibal and Ernst, 1965; Hiller, 1968; Gennaro, 1969; Stork, 1980; Autumn et al., 2000, 2002; Bergmann and Irschick, 2005; Huber et al., 2005b); and adhesive strength (Hiller, 1968; Irschick et al., 1996; Autumn et al., 2000; Arzt et al, 2003; Huber et al., 2005a, 2005b). There is great interest among the scientific community to further study the characteristics of gecko feet in hope that this information could be applied to the production of micro/nanosurfaces capable of recreating the adhesive forces generated by these lizards. Common man-made adhesives such as tape or glue involve the use of wet adhesives that permanently attach two surfaces. However, replication of the characteristics of gecko feet would enable the development of a super adhesive polymer tape capable of clean, dry adhesion (e.g. Geim et al., 2003; Sitti, 2003; Sitti and Fearing, 2003a, 2003b; Northen and Turner, 2005a, 2005b; Yurdumakan et al., 2005). These reusable adhesives have potential for use in everyday objects such as tape, fasteners, and toys (e.g. Full et al., 2004) and in high technology such as microelectric and space applications (e.g. Northen

and Turner, 2005a; Yurdumakan et al., 2005). Replication of the dynamic climbing and peeling ability of geckos could find use in the treads of wall-climbing robots (Sitti and Fearing, 2003b; Menon et al., 2004).

2.1 Tokay Gecko

2.1.1 Construction of Tokay Gecko

The explanation for the adhesive properties of gecko feet can be found in the surface structure of the skin on the toes of the gecko. The skin is comprised of a complex fibrillar structure of lamellae (scansors), setae, branches, and spatulae (Ruibal and Ernst, 1965). As shown in Figure 1(Autumn et al., 2000; Gao et al., 2005; Autumn, 2006) and schematically in Figure 2, the gecko consists of an intricate hierarchy of structures beginning with lamellae, soft ridges that are 1-2 mm in length (Ruibal and Ernst, 1965) that are located on the attachment pads (toes) that compress easily so that contact can be made with rough bumpy surfaces. Tiny curved hairs known as setae extend from the lamellae. These setae are typically 30-130 μm in length and 5-10 μm in diameter (Ruibal and Ernst, 1965; Hiller, 1968; Russell, 1975; Williams and Peterson, 1982). At the end of each seta, 100 to 1000 spatulae (Ruibal and Ernst, 1965; Hiller, 1968) with a diameter of 0.1-0.2 μm (Ruibal and Ernst, 1965) branch out and form the points of contact with the surface. The tips of the spatulae are are approximately 0.2-0.3 μm in width (Ruibal and Ernst, 1965) 0.5 μm in length and 0.01 μm in thickness (Persson and Gorb, 2003).

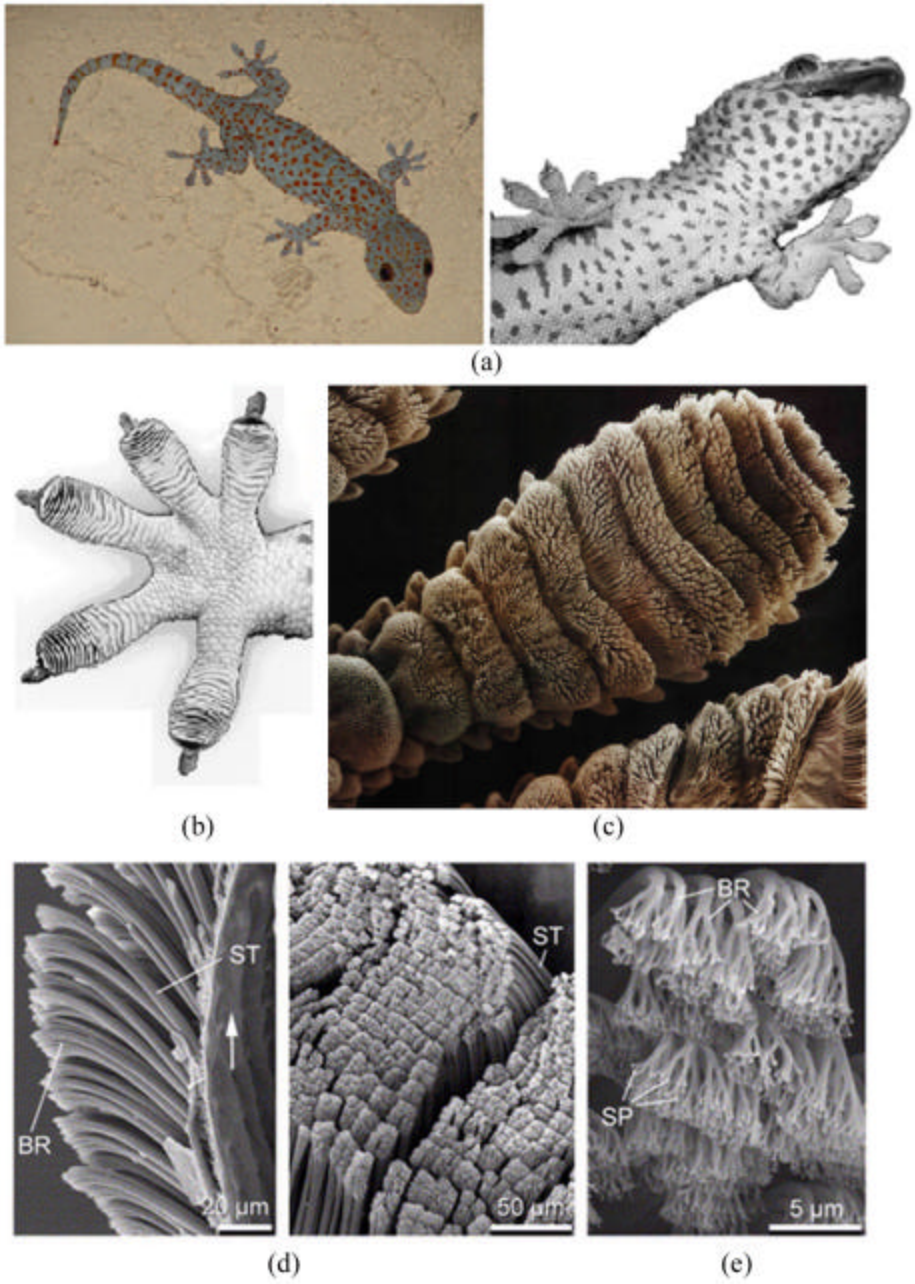

Fig. 1 (a) Photographs of a Tokay gecko. The hierarchical structures of a gecko foot; photographs of (b) a gecko foot and (c) a gecko toe. Each toe contains hundreds of thousands of seta and each seta contains hundreds of spatulae. (d) SEM micrographs of the seta and (e) spatulae, ST: seta; SP: spatulae; BR: branch.

Table 1 - Surface characteristics of Tokay gecko feet (Young's modulus of surface material, keratin = 1-20 GPa[1,2])

Component	Size	Density	Adhesive force
Seta	30-130[3-6] / 5-10[3-6] length/diameter (μm)	~14000[8,9] setae/mm^2	194 μN[10]
Branch	20-30[3] / 1-2[3] length/diameter (μm)	-	-
Spatula	2-5[3] / 0.1-0.2[3,7] length/diameter (μm)	100-1000[3,4] spatulae per seta	-
Tip of spatula	~0.5[3,7] / 0.2-0.3[3,6] /~0.01[7] length/width/thickness (μm)	-	11 nN[11]

[1] Russell (1986); [2] Bertram and Gosline (1987); [3] Ruibal and Ernst (1965); [4] Hiller (1968); [5] Russell (1975); [6] Williams and Peterson (1982); [7] Persson and Gorb (2003); [8] Schleich and Kästle (1986); [9]Autumn and Peattie (2002); [10] Autumn et al. (2000); [11] Huber et al. (2005a).

Several studies have been conducted to determine the number and size of the setae and spatulae of the gecko. Scanning electron microscopy has been employed to visually determine these values listed in Table 1. The setal density was originally reported to be 5,000 setae/mm^2 by Ruibal and Ernst (1965). This value has been used in various scientific studies (Autumn et al., 2000). Based on pictures obtained with a scanning electron microscope (SEM), a more accurate value of about 14,000 setae/mm^2 has been proposed by Schleich and Kästle (1986) and verified by Autumn and Peattie (2002). The attachment pads on two feet of the Tokay gecko have an area of about 220 mm^2, which can produce a clinging ability of about 20 N (vertical force required to pull a lizard down a nearly vertical (85°) surface) (Irschick et al., 1996).

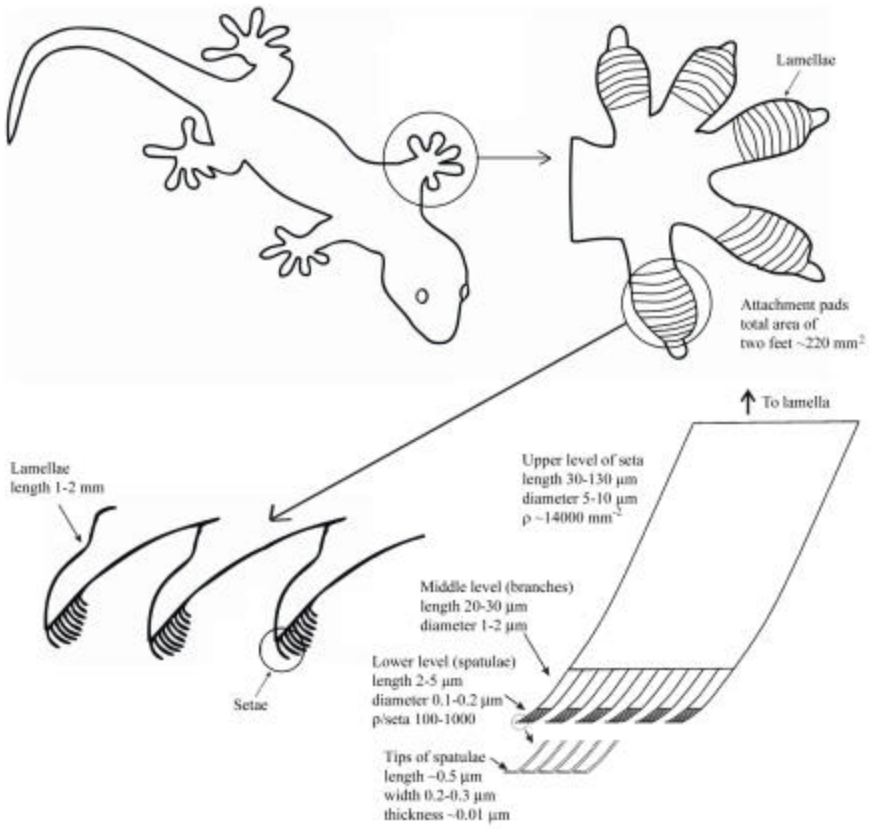

Fig. 2 Schematic drawings of a Tokay gecko including the overall body, one foot, a cross-sectional view of the lamellae, and an individual seta.

2.1.2 Other Attachment Systems

Attachment systems in other creatures such as insects and spiders have similar structures to that of gecko skin. The microstructures utilized by beetles, flies, spiders and geckos can be seen in Figure 3a. As the size (mass) of the creature increases, the radius of the terminal attachment elements decreases. This allows a greater number of setae to be packed into an area, hence increasing the real area of contact and the adhesive strength. It was determined by Arzt et al. (2003) that the density of the terminal attachment elements, $?_A$, per m^{-2} strongly increases with increasing body mass, m, in kg. In fact, a master curve can be fit between all the different species (Figure 3b).

$$\log ?_A = 13.8 + 0.669 \cdot \log m \qquad (1)$$

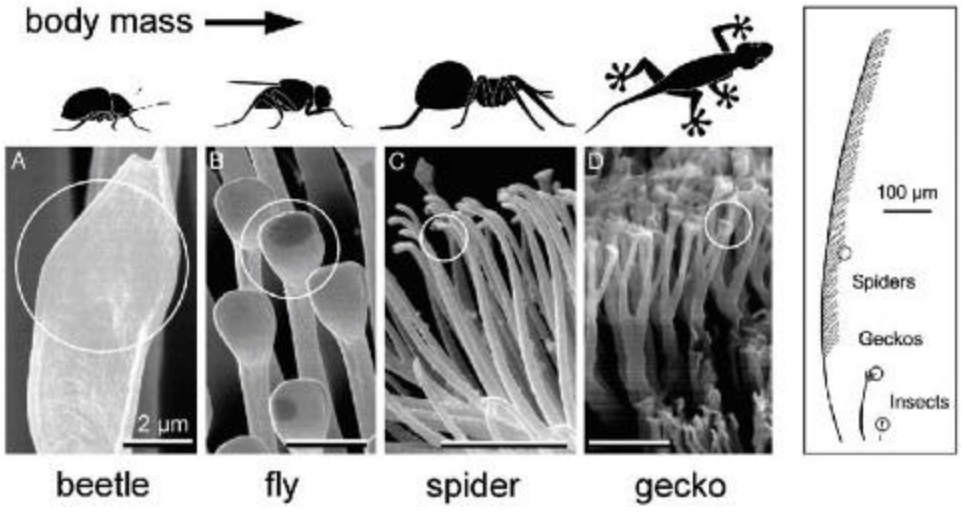

Fig. 3 (a) Terminal elements of the hairy attachment pads of a beetle, fly, spider, and gecko

The correlation coefficient, r, of the master curve is equal to 0.919. Flies and beetles have the largest attachment pads and the lowest density of terminal attachment elements. Spiders have highly refined attachment elements that cover the leg of the spider. Lizards have both the highest body mass and greatest density of terminal elements (spatulae).

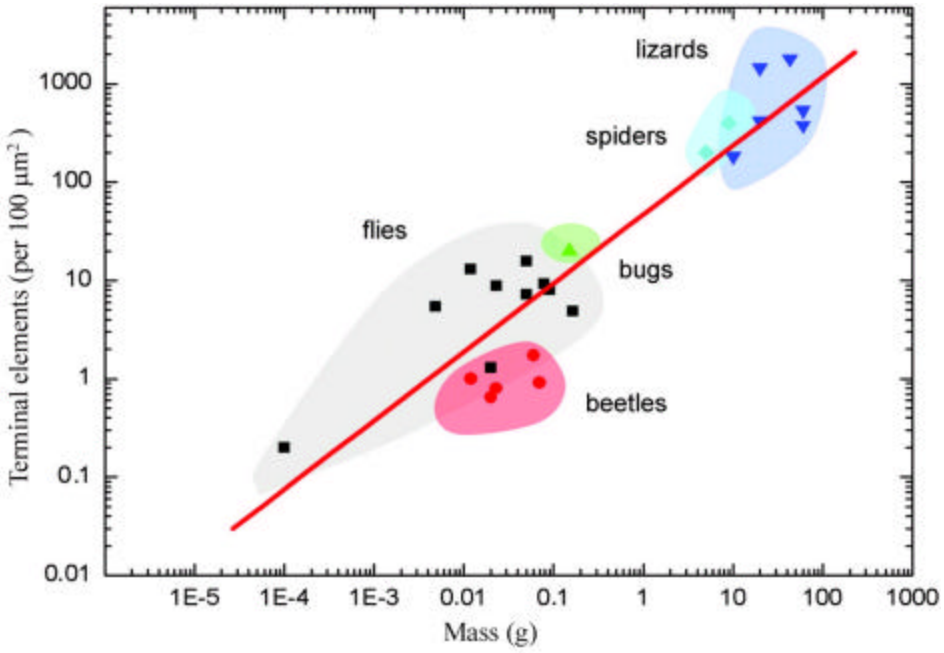

Fig. 3b The dependence of terminal element density on body mass (Arzt et al., 2003).

2.1.3 Adaptation to Surface Roughness

Typical rough, rigid surfaces are only able to make intimate contact with a mating surface equal to a very small portion of the perceived apparent area of contact. In fact, the real area of contact, A_r, is typically two to six orders of magnitude less than the apparent area of contact, A_a (Bhushan, 2002, 2005). Autumn et al. (2002) proposed that divided contacts serve as a means for increasing adhesion. Arzt et al. (2003) used a thermodynamical surface energy approach to calculate adhesive force. The authors

assumed that a spatula is a hemisphere with radius, *R*. For calculation of adhesive force of a single contact, F_a, a so called JKR (Johnson-Kendall-Roberts) theory was used (Johnson et al. 1971)

$$F_a = -(3/2)\pi g R \qquad (2)$$

where g is surface energy per unit area. Equation 2 shows that adhesive force of a single contact is proportional to a linear dimension of the contact. For a constant area divided into a large number of contacts or setae, n, the radius of a divided contact, R_1, is given by $R_1 = R/\sqrt{n}$. Therefore, the adhesive force of Equation 2 can be modified for multiple contacts such that

$$F_a^{'} = -(3/2)\pi g \left(R/\sqrt{n}\right) n = \sqrt{n} F_a \qquad (3)$$

where F_a' is the total adhesive force from the divided contacts. Thus the total adhesive force is simply the adhesive force of a single contact multiplied by the square root of the number of contacts. However, this model only considers contact with a flat surface.

On natural rough surfaces the compliance and adaptability of setae are the primary sources of high adhesion. Intuitively, the hierarchical structure of gecko setae allows for greater contact with a natural rough surface than non-branched attachment system. Two-dimensional profiles of surfaces that a gecko may encounter were obtained using a stylus profiler. These profiles along with the surface selection methods and

surface parameters for scan lengths of 80, 400, and 2000 μm are presented in Appendix A. Bhushan et al. (2006) used the spring model of Figure 4 to simulate the contact between a gecko seta and random rough surfaces similar to those found in Appendix A. The results of this model suggest that as levels of hierarchy are added to a surface, the adaptation range to roughness of that surface increases. The lamellae can adapt to the waviness of the surface while the setae and spatulae allow for the adaptation to micro and nanoroughness, respectively. Through the use of the hierarchy of structures of its skin, a gecko is able to bring a much larger percentage of its skin in contact with the mating surface.

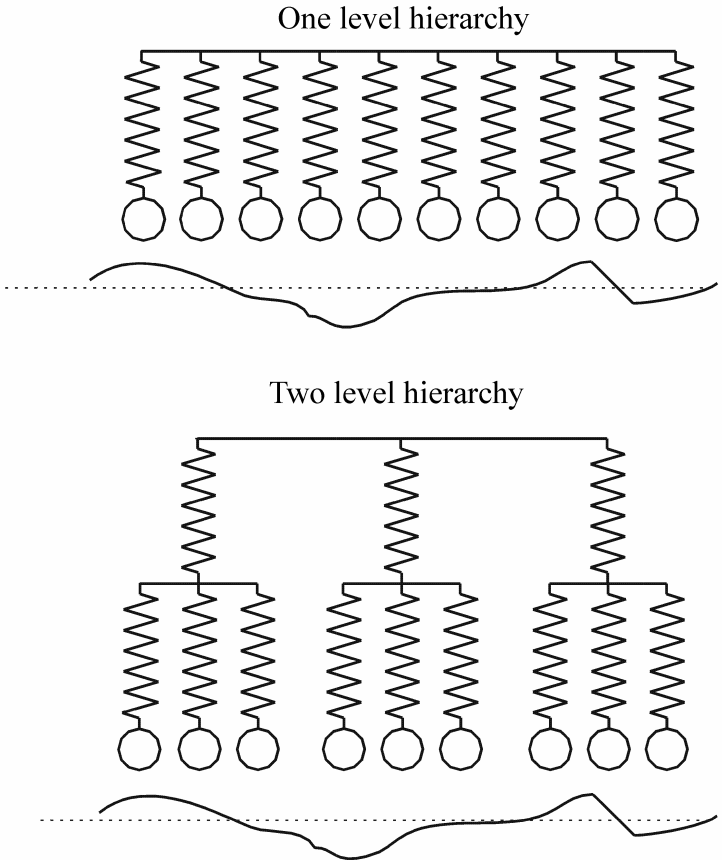

Fig. 4 One and two level spring models for the simulation of a seta of a Tokay gecko in contact and a random rough surface (Bhushan et al., 2006).

Material properties also play an important role in adhesion. A soft material is able to achieve greater contact with a mating surface than a rigid material (see Section 5.2). Gecko skin is comprised of ß-keratin, which has a Young's modulus in the range of 1-20 GPa (Russell, 1986; Bertman and Gosline, 1987). Gecko setae have a Young's modulus much lower than that of the bulk material. Autumn (2006) has experimentally determined that setae have an effective modulus of about 100 kPa. By combining optimal surface structure and material properties, Mother Nature has created an evolutionary superadhesive.

2.1.4 Peeling

Although geckos are capable of producing large adhesive forces, they retain the ability to remove their feet from an attachment surface at will. Autumn et al. (2000) were the first to experimentally show that adhesive force of gecko setae is dependent on the three dimensional orientation as well as the preload applied during attachment (see Section 4.1.1). Due to this fact, geckos have developed a complex foot motion during walking. First the toes are carefully uncurled during attachment. The maximum adhesion occurs at an attachment angle of 30º—the angle between a seta and mating surface. The gecko is then able to peel its foot from surfaces one row of setae at a time by changing the angle at which its setae contact a surface. At an attachment angle greater than 30º the gecko will detach from the surface.

Shah and Sitti (2004) determined the theoretical preload required for adhesion as well as the adhesive force generated for setal orientations of 30º, 40º, 50º, and 60º. In

order for a solid material (elastic modulus, E, Poisson's ratio, ?) to make contact with the rough surface described by

$$f(x) = h\sin^2\left(\frac{px}{l}\right) \tag{4}$$

where h is the amplitude and ? is the wavelength of the roughness profile. For a solid adhesive block to achieve intimate contact with the rough surface neglecting surface forces, it is necessary to apply a compressive stress, S_c, of (Jagota and Bennison, 2002)

$$S_c = \frac{pEh}{2\left(1-n^2\right)l} \tag{5}$$

Equation 5 can be modified to account for fibers oriented at an angle, ?. The preload required for contact is summarized in Figure 5a. As the orientation angle decreases, so does the required preload. Similarly, adhesive strength is influenced by fiber orientation. As seen in Figure 5b, the greatest adhesive force occurs at ? = 30º.

Gao et al. (2005) created a finite element model of a single gecko seta in contact with a surface. A tensile force was applied to the seta at various angles, ?, as shown in Figure 5c. For forces applied at an angle less than 30°, the dominant failure mode was sliding. On the contrary, the dominant failure mode for forces applied at angles greater than 30° was detachment. This verifies the results of Autumn et al. (2000) that detachment occurs at attachment angles greater than 30º.

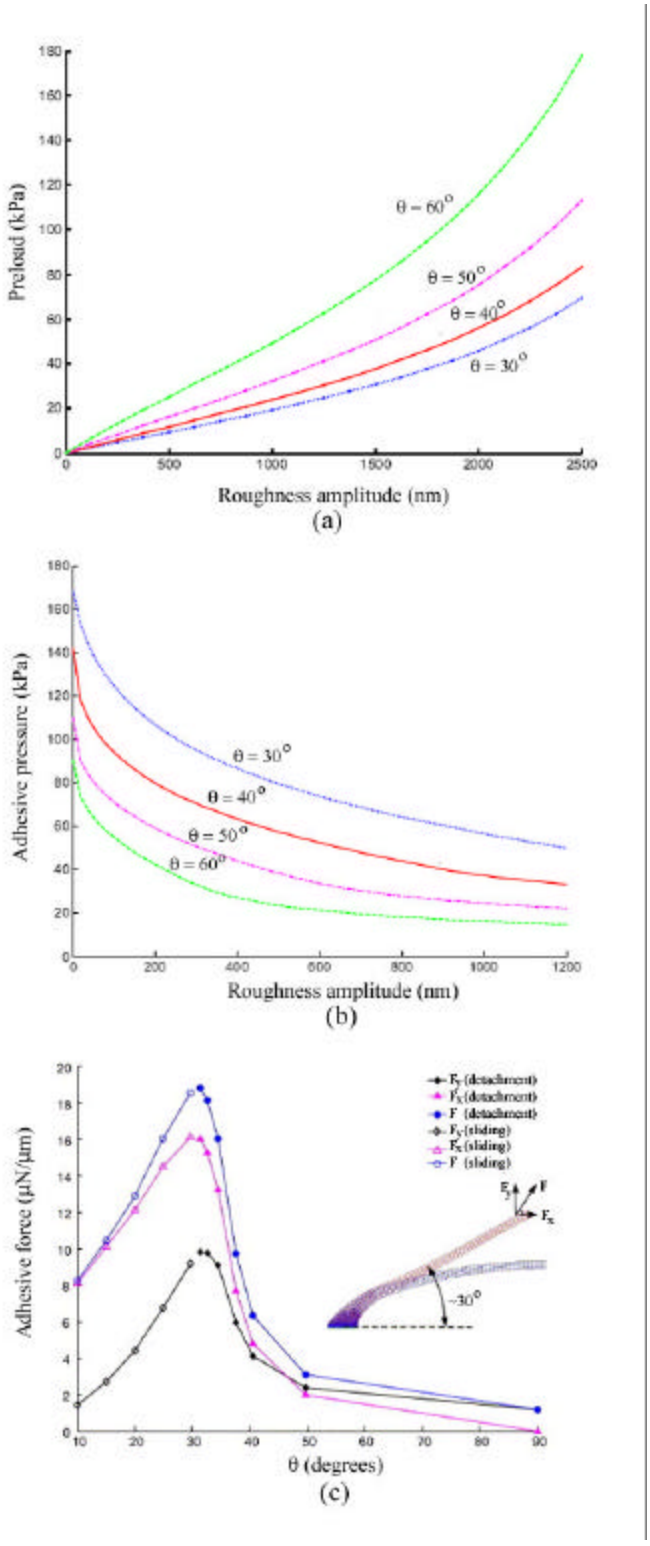

Fig. 5 Contact mechanics results for the affect of fiber orientation on (a) preload and (b) adhesive force for roughness amplitudes ranging from 0-2500 nm (Shah and Sitti, 2004). (c) Finite element analysis of the adhesive force of a single seta as a function of pull direction (Gao et al., 2005).

2.1.5 Self Cleaning

Intuitively, it seems that the great adhesive strength of gecko feet would cause dust and other particles to become trapped in the spatulae and have no way of being removed without some sort of manual cleaning action on the part of the gecko. However, geckos are not known to groom. One potential source of cleaning is during the time when the lizards undergo molting, or the shedding of the superficial layer of epidermal cells. However, this process only occurs approximately once per month (Van der Kloot, 1992). If molting were the sole source of cleaning, the gecko would rapidly lose its adhesive properties as it is exposed to contaminants in nature (Hansen and Autumn, 2005). Natural contaminants (dirt and dust) as well as man-made pollutants are unavoidable and have the potential to interfere with the clinging ability of geckos. Particles found in the air consist of particulates that are typically less than 10 μm in diameter while those found on the ground can often be larger (Hinds, 1982; Jaenicke, 1998). Geckos are not known to groom their feet like beetles (Stork, 1983) nor do they secrete sticky fluids to remove adhering particles like ants (Federle et al., 2002) and tree frogs (Hanna and Barnes, 1991), yet they retain adhesive properties. Hansen and Autumn (2005) tested the hypothesis that gecko setae become cleaner with repeated use—a phenomenon known as self-cleaning.

The cleaning ability of gecko feet was first tested experimentally. The test procedures employed by Hansen and Autumn (2005) will be summarized. For complete details see the reference. 2.5 μm radius silica-alumina ceramic microspheres were applied to clean setal arrays. Figure 6a shows the setal arrays immediately after dirtying and after five simulated steps. It can be noticed that a significant fraction of the particles

has been removed after five steps as compared to the original dirtied arrays. The maximum shear stress that these "dirty" arrays could withstand was measured using a piezoelectric force sensor. After each step that the gecko took, the shear stress was once again measured. As seen in Figure 6b, after only four steps, the gecko foot is clean enough to withstand its own body weight.

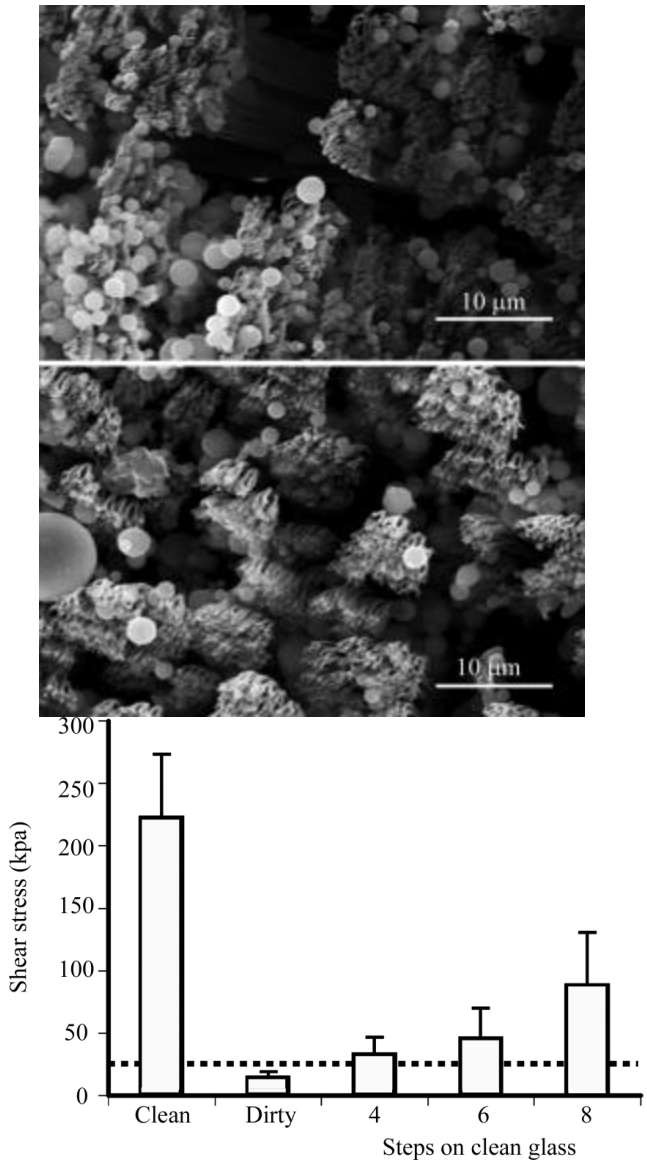

Fig. 6 (a) SEM images of spatulae (top) after dirtying with microspheres and (bottom) after five simulated steps. (b) Mean shear stress exerted by a gecko on a surface after dirtying. The dotted line represents sufficient recovery to support body weight by a single toe. (Hansen and Autumn, 2005).

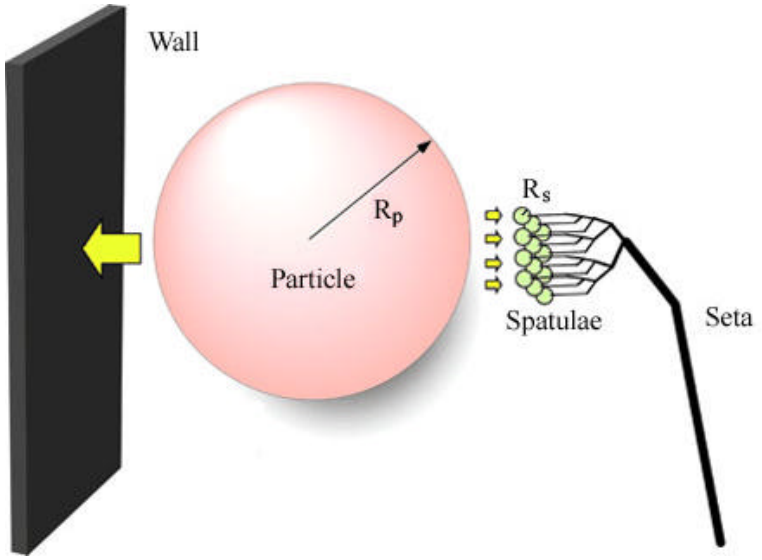

Fig. 7 Model of interactions between gecko spatulae of radius R_s, a spherical dirt particle of radius R_p, and a planar wall that enable self cleaning (Hansen and Autumn, 2005).

In order to understand this cleaning process, substrate-particle interactions must be examined. The interaction energy between a dust particle and a wall and spatulae can be modeled as shown in Figure 7. The interaction between a spherical dust particle and the wall, W_{pw}, can be expressed as (Israelachvili, 1992)

$$W_{pw} = \frac{-A_{pw} R_p}{6 D_{pw}} \tag{6}$$

where p and w refer to the particle and wall, respectively. A is the Hamaker constant, R_p is the radius of the particle, and D_{pw} is the separation distance between the particle and the wall. Similarly, the interaction energy between a spherical dust particle and a spatula, s, assuming that the spatula tip is spherical is (Israelachvili, 1992)

$$W_{ps} = \frac{-A_{ps} R_p R_s}{6 D_{ps} (R_p + R_s)} \tag{7}$$

The ratio of the two interaction energies, N, can be expressed as

$$N = \frac{W_{pw}}{W_{ps}} = \left(1 + \frac{R_p}{R_s}\right) \frac{A_{pw} D_{ps}}{A_{ps} D_{pw}} \tag{8}$$

When the energy required to separate a particle from the wall is greater than that required to separate it from a spatula, self-cleaning will occur. For example, if R_p = 2.5 μm and R_s = 0.1 μm (Ruibal and Ernst, 1965; Williams and Peterson, 1982), self cleaning will occur as long as no more than 26 spatulae are attached to the dust particle at one time assuming similar Hamaker constants and gap distances. The maximum number of spatulae, as well as the percentage of available spatulae, in contact with a particle for self-cleaning to occur is tabulated in Table 2. It can be seen that very small particles (<0.5 μm diameter)

Table 2 – Maximum number of spatulae that can be in contact with a contaminant particle in order for self cleaning to occur (spatula radius, R_s, is 0.1 μm).

Radius of particle (μm)	Maximum no. of spatulae in contact with particle	Area of sphere (μm^2)	spatulae available	% needed to adhere
0.1	2	0.03	0.25	804%
0.5	6	0.79	6.2	96%
1	11	3	25	44%
2.5	26	19	156	17%
5	51	79	622	8%
10	101	314	2488	4%
20	201	1257	9952	2%

do not come into contact with enough spatulae to adhere. Due to the curvature of larger particles relative to the planar field of the spatulae, very few spatulae are able to come into contact with the particle. As a result, Hansen and Autumn (2005) concluded that self-cleaning should occur for all spherical spatulae interacting with all spherical particles.

2.2 Attachment Mechanisms

When asperities of two solid surfaces are brought into contact with each other, chemical and/or physical attractions occur. The force developed that holds the two surfaces together is known as adhesion. In a broad sense, adhesion is considered to be either physical or chemical in nature (Bikerman, 1961; Zisman, 1963; Houwink and Salomon, 1967; Israelachvili , 1992; Bhushan, 1996, 1999, 2002, 2005). Chemical interactions such as electrostatic attraction charges (Schmidt, 1904) as well as physical interactions such as capillary forces (Hiller, 1968) and van der Waals forces (Hiller, 1968) have all been proposed as potential adhesion mechanisms in gecko feet. Others have hypothesized that geckos adhere to surfaces through the secretion of sticky fluids (Wagler, 1830; Simmermacher, 1884), suction (Simmermacher, 1884), increased frictional force (Hora, 1923), and microinterlocking (Dellit, 1934).

2.2.1 Unsupported Adhesive Mechanisms

Several of the aforementioned mechanisms have been unsupported in testing. The rejected mechanisms of adhesion are summarized in Table 3a.

Table 3 – Proposed mechanisms of adhesion utilized by gecko feet and experimental evidence (a) against and (b) in favor of the proposed theories.

(a) Unsupported Adhesive Mechanisms

Mechanism	Proposed by	Experimental evidence against	Disproven by
Secretion of sticky fluids	N/A	Geckos lack glands on their toes that produce sticky fluids capable of adhesion	Wagler (1830); Simmermacher (1884)
Suction	Simmermacher (1884)	The adhesive force of a gecko is not affected in high vacuum experiments.	Dellit (1934)
Electrostatic attraction	Schmidt (1904)	Geckos are able to adhere to surfaces in ionized air (which would eliminate electrostatic attraction).	Dellit (1934)
Increased frictional force	Hora (1923)	Observations that a gecko can adhere upside down, even though friction force only acts parallel to a surface.	Numerous observers
Microinterlocking	Dellit (1934)	Measurements of large of adhesive forces of a gecko seta on molecularly smooth SiO_2	Autumn et al. (2000)

(b) Supported Adhesive Mechanisms

Mechanism	Proposed by	Experimental evidence for	Supported by
van der Waals forces (Primary)	Hiller (1968)	Overall and setal adhesion matches the theoretical adhesion values predicted by van der Waals forces.	Autumn et al. (2000)
Capillary forces (Secondary)	Hiller (1968)	Adhesive force of a single gecko spatula was affected by relative humidity present in the air.	Huber et al. (2005b)

2.2.1.1 Secretion of Sticky Fluids

Although several insects and frogs rely on sticky fluids to adhere to surfaces, geckos lack glands on their toes capable of producing these fluids (Wagler, 1830; Simmermacher, 1884). As a result, this hypothesis has been ruled out.

2.2.1.2 Suction

Simmermacher (1884) proceeded to propose that geckos make use of miniature suction cups as an adhesive mechanism. Suction cups operate under the principle of microcapillary evacuation (MCE). When a suction cup comes into contact with a

surface, air is forced out of the contact area creating a pressure differential. The adhesive force generated is simply the pressure differential multiplied by the apparent area of contact (Bhushan, 1996).

Suction cups lose their adhesive strength when used under high vacuum conditions since a pressure differential can no longer be developed. This mechanism of adhesion can be easily investigated by comparing adhesive force under vacuum to adhesive force at atmospheric conditions. Experiments carried out in vacuum by Dellit (1934) did not show a difference between the adhesive force at these conditions compared to ambient conditions, thus rejecting suction as an adhesive mechanism.

2.2.1.3 Electrostatic Attraction

Electrostatic attraction occurs when two dissimilar heteropolar surfaces come in contact. Electrostatic forces are produced by one or more valence electrons transferring completely from one atom to another. When the separation between two surfaces is approximately equal to atomic spacing (0.3 nm), the bond generated is quite strong and resembles that within the bulk material. If an insulator (e.g. gecko setae) is brought into contact with a metal, there is a large separation of charge at the interface that produces an electrostatic attraction (Johnsen and Rahbek, 1923; Skinner et al., 1953; Davies, 1973; Wahlin and Backstrom, 1974; Derjaguin et al., 1978). Rubbing action during activities such as walking and running would increase the fraction of charged surface area. This is often referred to as the "triboelectric" effect (Shaw, 1923; Henry, 1953).

Schmidt (1904) proposed electrostatic attraction as the mechanism of adhesion used by the gecko attachment system. Dellit (1934) conducted experiments to determine

the electrostatic contribution to gecko adhesion. This testing utilized X-ray bombardment to create ionized air and hence eliminate electrostatic attraction. It was determined that geckos were still able to adhere to surfaces in these conditions and therefore, electrostatic charges could not be the sole cause of attraction.

2.2.1.4 Increased Frictional Force

It has also been postulated that adhesive strength of gecko attachment pads arise from high friction force due to a large real area of contact (Hora, 1923). The hierarchical structure of lamellae-setae-branches-spatulae enable a gecko to create a real area of contact with a mating surface that is orders of magnitude greater than a non divided surface. Since the coefficients of static and kinetic friction are dependent contact area (Bhushan, 2002, 2005), a large real area of contact would cause a large coefficient of friction. Under this theory a gecko would be able to climb vertical walls if the frictional force exceeded the weight of the lizard. Although large frictional forces could enable geckos to walk up vertical surfaces, it would not account for a gecko's ability to cling to surfaces upside down. Friction force only acts in the direction parallel to the contact surface, yet to hang upside down an adhesive force is required perpendicular to the surface. As a result, frictional force has been discounted as a potential mechanism.

2.2.1.5 Microinterlocking

Dellit (1934) proposed that the curved shape of setae act as microhooks that catch on rough surfaces. This process known as microinterlocking would allow geckos to attach to rough surfaces. Autumn et al. (2000) demonstrated the ability of a gecko

generate large adhesive forces when in contact with a molecularly smooth SiO_2 MEMS semiconductor. Since surface roughness is necessary for microinterlocking to occur, it has been ruled out as a mechanism of adhesion.

2.2.2 Supported Adhesive Mechanisms

Two mechanisms, van der Waals forces and capillary forces, remain as the potential sources of gecko adhesion. These attachment mechanisms are described in detail in the proceeding sections and summarized in Table 3b.

2.2.2.1 van der Waals Forces

van der Waals bonds are secondary bonds that are weak in comparison to other physical bonds such as covalent, hydrogen, ionic, and metallic bonds. Unlike other physical bonds, van der Waals forces are always present regardless of separation and are effective from very large separations (~50 nm) down to atomic separation (~0.3 nm). The van der Waals force per unit area between two parallel surfaces, f_{vdW}, is given by (Hamaker, 1937; Israelachvili and Tabor, 1972; Israelachvili, 1992)

$$f_{vdW} = \frac{A}{6p\,D^3} \qquad \text{for} \qquad D < 30 \text{ nm} \tag{9}$$

where A is the Hamaker constant and D is the separation between surfaces.

Hiller (1968) proposed that van der Waals forces as a potential adhesive mechanism. Assuming van der Waals forces to be the dominant adhesive mechanism

utilized by geckos, the adhesive force of a gecko can be calculated. Typical values of the Hamaker constant range from $4x10^{-20}$ to $4x10^{-19}$ J (Israelachvili, 1992). In calculation, the Hamaker constant is assumed to be 10^{-19} J, the surface area of a spatula is taken to be $2x10^{-14}$ m^2 (Ruibal and Ernst, 1965; Williams and Peterson, 1982; Autumn and Peattie, 2002), and the separation between the spatula and contact surface is estimated to be 0.6 nm. This equation yields the force of a single spatula to be about 0.5 µN. By applying the surface characteristics of Table 1, the maximum adhesive force of a gecko is 150-1500 N for varying spatula density of 100-1000 spatulae per seta. If an average value of 550 spatulae/seta is used, the adhesive force of a single seta is approximately 270 µN which is in agreement with the experimental value obtained by Autumn et al. (2000), which will be discussed in Section 4.1.1.

Another approach to calculate adhesive force is to assume that spatulae are cylinders that terminate in hemispherical tips. By using Equation 2 and assuming that the radius of each spatula is about 100 nm and that the surface energy is expected to be 50 mJ/m^2 (Arzt et al., 2003), the adhesive force of a single spatula is predicted to be 0.02 µN. This result is an order of magnitude lower than the first approach calculated for the higher value of A. For a lower value of 10^{-20} J for the Hamaker constant, the adhesive force of a single spatula is comparable to that obtained using the surface energy approach.

Several experimental results favor van der Waals forces as the dominant adhesive mechanism including temperature testing (Bergman and Irschick, 2005) and adhesive force measurements of a gecko seta with both hydrophilic and hydrophobic surfaces (Autumn et al., 2000). This data will be presented in the Sections 4.2-4.4.

2.2.2.2 Capillary Forces

It has been hypothesized that capillary forces that arise from liquid mediated contact could be a contributing or even the dominant adhesive mechanism utilized by gecko spatulae (Hiller, 1968; Stork, 1980). Experimental adhesion measurements (presented in Sections 4.3 and 4.4) conducted on surfaces with different hydrophobicities and at various humidities (Huber et al., 2005b) supports this hypothesis as a contributing mechanism. During contact, any liquid that wets or has a small contact angle on surfaces will condense from vapor in the form of an annular-shaped capillary condensate. Due to the natural humidity present in the air, water vapor will condense to liquid on the surface of bulk materials. During contact this will cause the formation of adhesive bridges (menisci) due to the proximity of the two surfaces and the affinity of the surfaces for condensing liquid. (Zimon, 1969; Fan and O'Brien, 1975; Phipps and Rice, 1979).

Capillary forces can be divided into two components: a meniscus force from surface tension and a rate dependent viscous force (Bhushan, 1999, 2002, 2005). The total adhesive force is simply the sum of the two components. The meniscus contribution to adhesion between a spherical surface and a flat plate, F_M, is given by (McFarlane and Tabor, 1950)

$$F_M = 2\pi R\gamma_l(\cos\theta_1 + \cos\theta_2) \quad (10)$$

where R is the radius of the sphere, γ_l is the surface tension of the liquid, and θ_1 and θ_2 are the contact angles of the sphere and plate, respectively. It should be noted that meniscus force is independent of film thickness. Consequently, even a film as thin as a

single monolayer can significantly influence the attraction between two surfaces (Israelachvili, 1992; Bhushan, 1996, 2002).

The viscous component of liquid-mediated adhesion is given by (McFarlane and Tabor, 1950)

$$F_v = \frac{b h_l}{t_s} \tag{11}$$

where ß is a proportionality constant, ?$_l$ is the dynamic viscosity of the liquid, and t_s is the time to separate the two surfaces. t_s is inversely related to velocity of the interface during detachment. Furthermore, the fluid quantity has a weak dependence on viscous force.

2.3. Experimental Adhesion Test Techniques and Data

Experimental measurements of the adhesive force of a single gecko seta (Autumn et al., 2000) and single gecko spatula (Huber et al., 2005a, 2005b) have been made. The effect of the environment including temperature (Losos, 1990; Bermann and Irschick, 2005) and humidity (Huber et al., 2005b) has been studied. Some of the data has been used to understand the adhesive mechanism utilized by the gecko attachment system—van der Waals or capillary forces. The majority of experimental results point towards van der Waals forces as the dominant mechanism of adhesion (Autumn et al., 2000, Bergmann and Irschick, 2005). Recent research suggests that capillary forces can be a contributing adhesive factor (Huber et al., 2005b).

2.3.1 Adhesion under Ambient Conditions

Two feet of a Tokay gecko are capable of producing about 20 N of adhesive force with a pad area of about 220 mm^2 (Irschick et al., 1996). Assuming that there are 14400 setae per mm^2, the adhesive force from a single hair should be approximately 7μN. It is likely that the magnitude is actually greater than this value because it is unlikely that all setae are in contact with the mating surface (Autumn et al., 2000). Setal orientation greatly influences adhesive strength. This dependency was first noted by Autumn et al. (2000). It was determined that the greatest adhesion occurs at 30º. In order to determine the adhesive mechanism(s) utilized by gecko feet, it is important to know the adhesive force of a single seta. Hence, the adhesive force of gecko foot-hair has been the focus of several investigations (Autumn et al., 2000; Huber et al., 2005a).

2.3.1.1 Adhesive Force of a Single Seta

Autumn et al. (2000) used both a microelectromechanical (MEMS) force sensor and a wire as a force gauge to determine the adhesive force of a single seta. The MEMS force sensor is a dual-axis atomic force microscope (AFM) cantilever with independent piezoresistive sensors which allows simultaneous detection of vertical and lateral forces (Chui et al., 1998). The wire force gage consisted of an aluminum bonding wire which displaced under a perpendicular pull. Autumn et al. (2000) discovered that setal force actually depends on the three-dimensional orientation of the seta as well as the preloading force applied during initial contact. Setae that were preloaded vertically to the surface exhibited only one-tenth of the adhesive force (0.6 ± 0.7 μN) compared to setae that were pushed vertically and then pulled horizontally to the surface (13.6 ± 2.6 μN). The

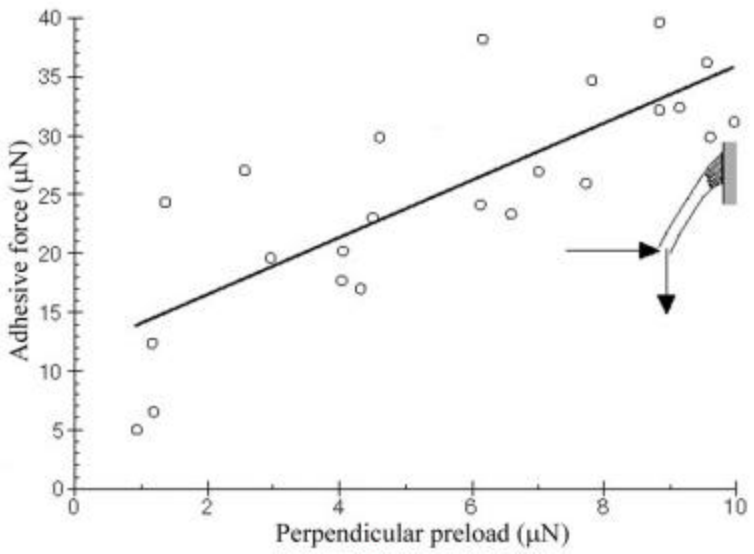

Fig. 8 Adhesive force of a single gecko seta as a function of applied preload. The seta was first pushed perpendicularly against the surface and then pulled parallel to the surface (Autumn et al., 2000).

dependence of adhesive force of a single gecko spatula on perpendicular preload is illustrated in Figure 8. The adhesive force increases linearly with the preload. The maximum adhesive force of a single gecko foot-hair occurred when the seta was first subjected to a normal preload and then slid 5 μm along the contacting surface. Under these conditions, adhesive force measured 194 ± 25 μN (~10 atm adhesive pressure).

2.3.1.2 Adhesive Force of a Single Spatula

Huber et al. (2005a) used atomic force microscopy to determine the adhesive force of individual gecko spatulae. A seta with four spatulae was glued to an AFM tip. The seta was then brought in contact with a surface and a compressive preload of 90 nN was applied. The force required to pull the seta off of the surface was then measured. As seen in Figure 9, there are two distinct peaks on the graph—one at 10 nN and the other at 20 nN. The first peak corresponds to one of the four spatulae adhering to the contact

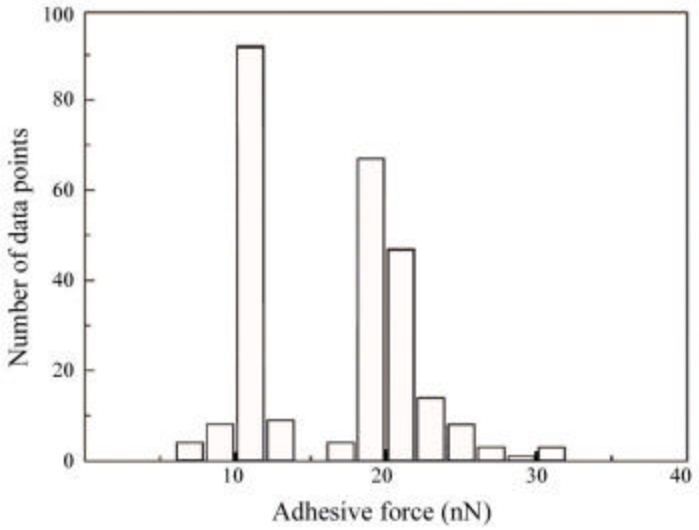

Fig. 9 Adhesive force of a single gecko spatula. The peak at 10 nN corresponds to the adhesive force of one spatula and the peak at 20 nN corresponds to the adhesive force of two spatulae (Huber et al., 2005a).

surface while the peak at 20 nN corresponds to two of the four spatulae adhering to the contact surface. The average adhesive force of a single spatula was found to be of 10.8 ± 1 nN. The measured value is in agreement with the measured adhesive strength of an entire gecko (10^9 spatulae on a gecko).

2.3.2 Effects of Temperature

Environmental factors are known to affect several aspects of vertebrate function, including speed of locomotion, digestion rate and muscle contraction, and as a result several studies have been completed to investigate environmental impact on these functions. Relationships between the environment and other properties such as adhesion are far less studied (Bergmann and Irschick, 2005). Only two known studies exist that examine the affect of temperature on the clinging force of the gecko (Losos, 1990; Bergmann and Irschick, 2005). Losos (1990) examined adhesive ability of large live

geckos at temperatures up to 17?C. Bergmann and Irschick (2005) expanded upon this research for body temperatures ranging from 15-35 ?C. The geckos were incubated until their body temperature reached a desired level. The clinging ability of these animals was then determined by measuring the maximum exerted force by the geckos as they were pulled off a custom-built force plate. The clinging force of a gecko for the experimental test range is plotted in Figure 10. It was determined that variation in temperature is not statistically significant in the adhesion force of a gecko. From these results, it was concluded that the temperature independence of adhesion supports the hypothesis of clinging as a passive mechanism (i.e. van der Waals forces). Both studies only measured overall clinging ability on the macroscale. There have not been any investigations into effects of temperature on the clinging ability of a single seta on the microscale and therefore testing in this area would be extremely important.

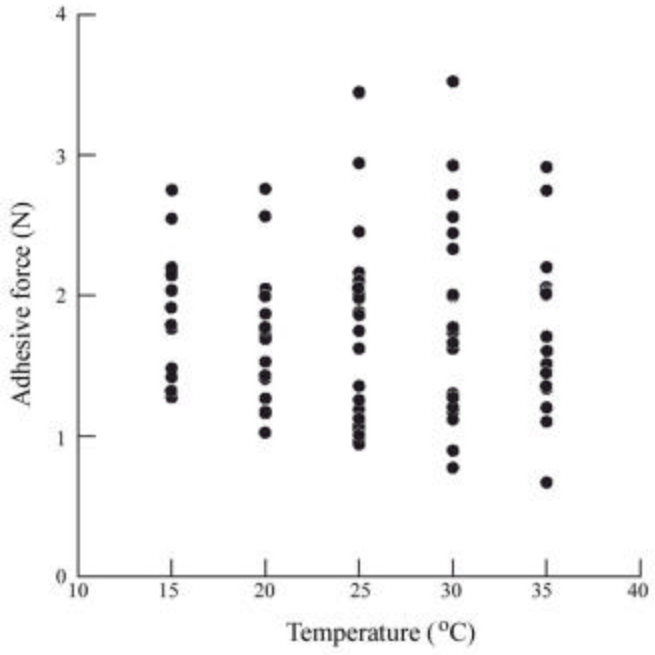

Fig. 10 Adhesive force of a gecko as a function of temperature (Bergmann and Irschick, 2005).

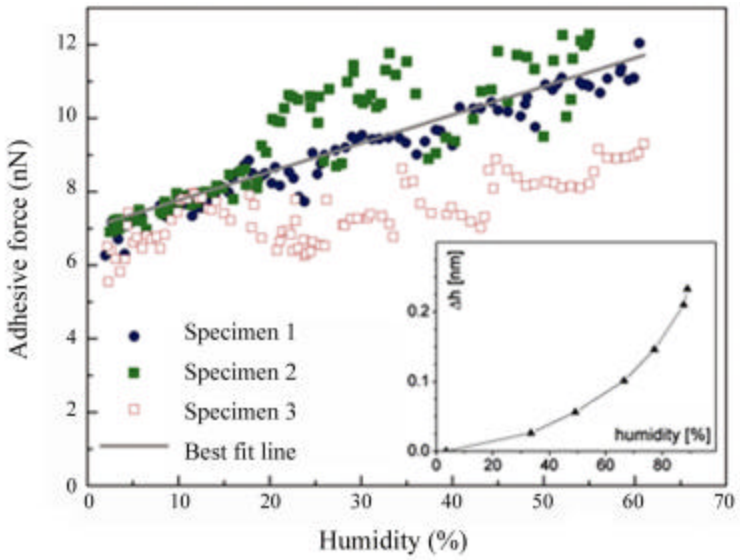

Fig. 11 Humidity effects on spatular pull-off force. (Inset) The increase in water film thickness on a Si wafer with increasing humidity (Huber et al., 2005b).

2.3.3 Effects of Humidity

Huber et al. (2005b) employed similar methods to Huber et al. (2005a) (discussed previously in Section 4.1.2) in order to determine the adhesive force of a single spatula at varying humidity. Measurements were made using an AFM placed in an air-tight chamber. The humidity was adjusted by varying the flow rate of dry nitrogen into the chamber. The air was continuously monitored with a commercially available hygrometer. All tests were conducted at ambient temperature.

As seen in Figure 11, even at low humidity, adhesive force is large. An increase in humidity further increases the overall adhesive force of a gecko spatula. The pull-off force roughly doubled as the humidity was increased from 1.5% to 60%. This humidity effect can be explained in two possible ways: (1) by standard capillarity or (2) by a change of the effective short-range interaction due to absorbed monolayers of water—in other words, the water molecules increase the number of van der Waals bonds that are

made. Based on this data, van der Waals forces are the primary adhesive mechanism and capillary forces are a secondary adhesive mechanism.

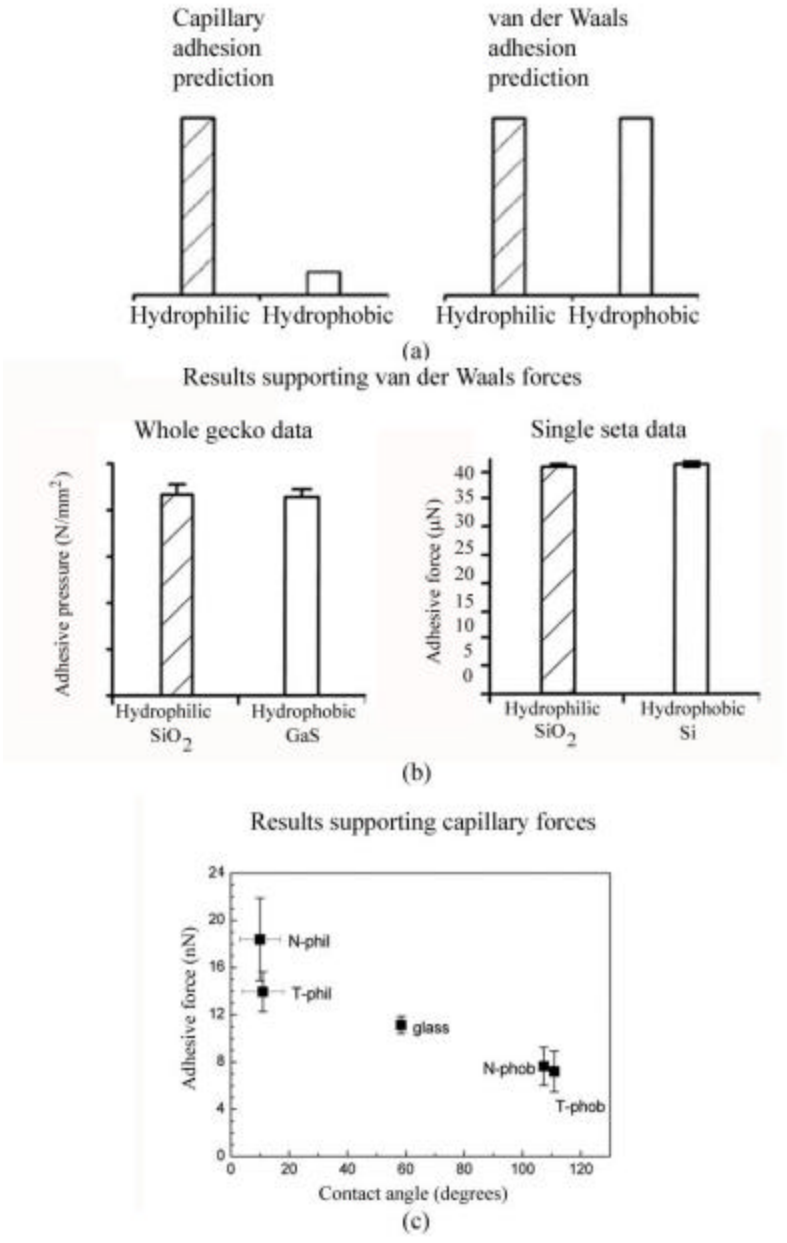

Fig. 12 (a) Capillary and van der Waals adhesion predictions for the relative magnitude of the adhesive force of gecko setae with hydrophilic and hydrophobic surfaces (Autumn et al., 2002). (b) Results of adhesion testing for a whole gecko and single seta with hydrophilic and hydrophobic surfaces (Autumn et al., 2002) and (c) results of adhesive force testing with surfaces with different contact angles (Huber et al., 2005b).

2.3.4 Effects of Hydrophobicity

To further test the hypothesis capillary forces, plays a role in gecko adhesion, the spatular pull-off force was determined for contact with both hydrophilic and hydrophobic surfaces. As seen in Figure 12a, the capillary adhesion theory predicts that a gecko spatula will generate a greater adhesive force when in contact with a hydrophilic surface as compared to a hydrophobic surface while the van der Waals adhesion theory predicts that the adhesive force between a gecko spatula and a surface will be the same regardless of the hydrophobicity of the surface (Autumn et al., 2002). Figure 12b shows the adhesive pressure of a whole gecko and adhesive force of a single seta on hydrophilic and hydrophobic surfaces. The data shows that the adhesive values are the same on both surfaces. This supports the van der Waals prediction of Figure 12a. Huber et al. (2005b) found that the hydrophobicity of the attachment surface had an effect on the adhesive force of a single gecko spatula as shown in Figure 12c. These results show that adhesive force has a finite value for superhydrophobic surface and increases as the surface becomes hydrophilic. It is concluded that van der Waals forces are the primary mechanism and capillary forces further increase the adhesive force generated.

2.4 Design of Biomimetic Fibrillar Structures

2.4.1 Verification of Adhesion Enhancement of Fabricated Surfaces using Fibrillar Structures

In order to create a material capable of dry adhesion, one would want to mimic the hierarchical structures found on the attachment pads of insects and lizards. Peressadko and Gorb (2004) investigated whether adhesion enhancement was experienced through a division of contact area or fibrillar structure. The adhesive strength of a patterned surface and a smooth surface (roughness amplitude, R_a = 0.5 nm) of polyvinylsiloxane (PVS) was tested on both a smooth and curved glass surface. Both PVS surfaces were molded. The patterned surface consisted of 72 columns (height = 400 µm, cross section 250 µm x 125 µm). The samples were loaded perpendicular to the glass surface. During unloading, the adhesive force was measured. As seen in Figure 13, the adhesive strength of the structured sample was several times greater than that of the flat sample. The adhesive strength of the fibrillar sample decreases at a load beyond 800 mN. This decline in adhesion is due to column buckling. Although the testing only dealt with surfaces made of PVS, one can assume that similar adhesion enhancement would result in structured samples of any material.

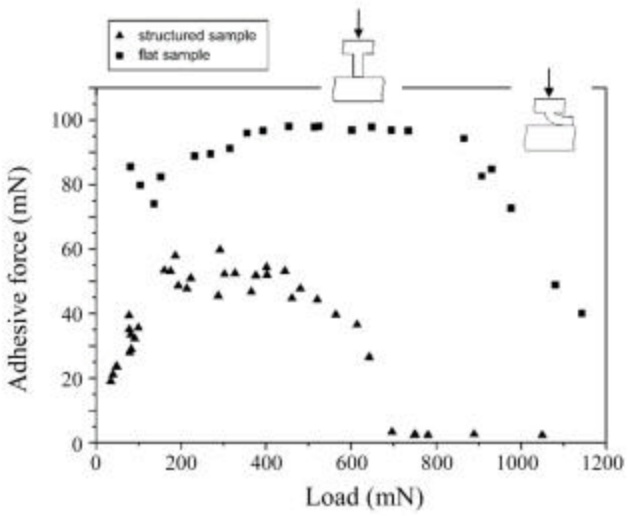

Fig. 13 Adhesive force of structured and flat PVS samples with a flat glass surface (Peressadko and Gorb, 2004).

2.4.2 Contact Mechanics of Fibrillar Structures

In order for a fibrillar microstructure to act as a good adhesive, it is necessary that the materials be compliant. This allows the fibrillar interface to make contact at as many points as possible. The mechanics of adhesion between a fibrillar structure and a rough surface have been a topic of investigation by many researchers (Jagota and Bennison, 2002; Persson, 2003; Sitti and Fearing, 2003a; Glassmaker et al., 2004, 2005; Gao et al., 2005). In order to better understand the mechanics of adhesion, the approach of Jagota and Bennison (2002) will be described. The fibrillar surface is modeled in two dimensions, as shown in Figure 14a, and is described by the length, L, and width, 2a, of the fibrils, and by the area fraction of the interface covered by fibril ends, f. Fibrils comprised of two different materials are investigated, a soft material and a hard material. Both of these materials are assumed to be linear elastic and have properties corresponding to those tabulated in Table 4.

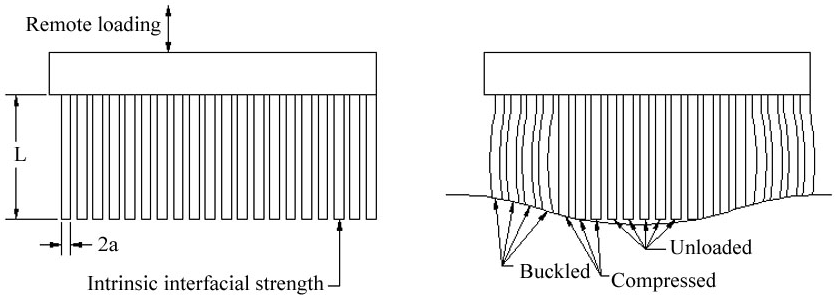

Fig. 14 (a) Geometry of a model fibrillar structure and (b) fibrillar mat loaded in compression against a rough surface.

If one wants to achieve intimate contact between an elastic solid and a wavy surface given by Equation 4, a compressive stress, S_c, must be applied to the surface. Intimate contact is achieved when (Hui et al., 2002)

$$\frac{pEh}{2(1-n^2)S_c l} < 1 \qquad (12)$$

where E is Young's modulus and ? is Poisson's ratio. By substituting the values of Table 4 into this equation, soft and hard materials can tolerate a surface roughness aspect ratios, h/?, of approximately $5x10^{-3}$ and $5x10^{-6}$, respectively.

Table 4 - Material properties for a soft, good adhesive and a stiff, weak adhesive (Jagota and Bennison, 2002).

Parameter	Soft, good adhesive	Stiff, weak adhesive
Young's modulus, E	10^6 Pa	10^9 Pa
Interfacial fracture energy, G_0	100 J/m^2	1 J/m^2
Interfacial strength, s'	10^6 Pa	10^3 Pa
Applied stress, s	10^4 Pa	10^4 Pa

If the fibrillar surface is to make contact with a rough surface, the fibrillar mat will be loaded as seen in Figure 14b. The buckling stress, S_b, is given by (Timoshenko and Gere, 1961)

$$\frac{S_b}{E} = \frac{1}{3} fp^2 \left(\frac{a}{L}\right)^2 \tag{13}$$

If f is taken to be 0.75, the width to length ratio, (a/L), must be less than or equal to 0.064 for the soft material and 0.002 for the hard material in order for uniform contact to occur.

When long, slender beams (such as setae or nanobumps) are in close proximity, the potential for two adjacent members to adhere laterally to each other arises as depicted in Figure 15. Hui et al. (2002) determined a relation to check for this phenomenon,

$$\frac{L}{2a}\left(\frac{2g_s}{3Ea}\right)^{1/4} < \left(\frac{w}{a}\right)^{1/2} \tag{14}$$

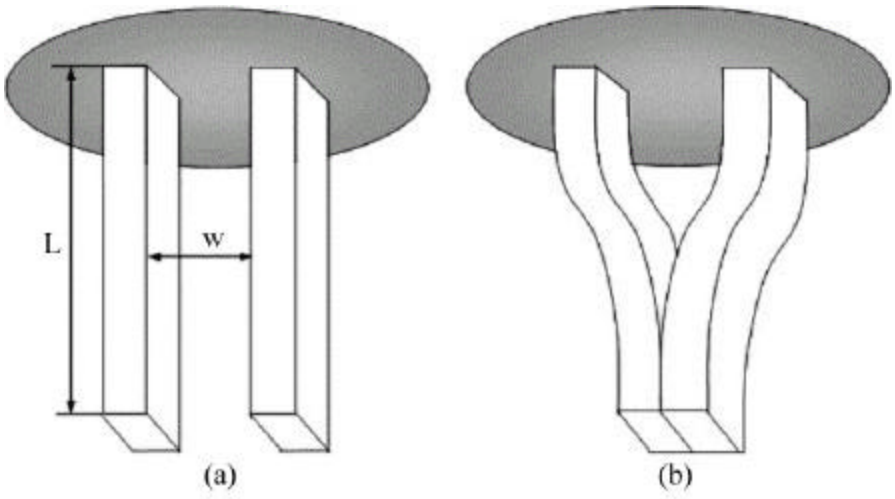

Fig. 15 Model of two adjacent fibers adhering laterally to each other (Gao et al., 2005).

where w is the gap between fibrils and $?_s$ is the surface energy (0.05 J/m^2). Assuming (w/a) to be 1, the width to length ratio must be greater than or equal to 0.25 and 0.045 for the soft and hard materials, respectively.

It is evident when comparing the results of Equations 13 and 14, that it is not possible for all of the fibrils to be in contact with the sinusoidal surface of Equation 4. As a result, there is a trade-off between the aspect ratio of the fibrils and their adaptability of a rough surface. If the fibrils aspect ratio is too large, they can adhere to each other or even collapse under their own weight as shown in Figure 16a. If the aspect ratio is too small (Figure 16b), the structures will lack the necessary compliance to conform to a rough surface.

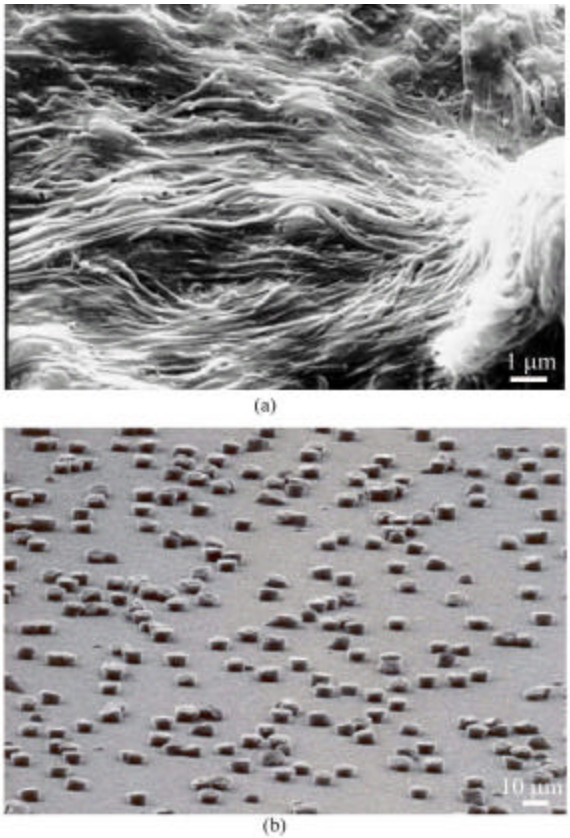

Fig. 16 SEM micrographs of (a) high aspect ratio polymer fibrils that have collapsed under their own weight and (b) low aspect ratio polymer fibrils that are incapable of adapting to rough surfaces (Sitti and Fearing, 2002).

2.4.3 Fabrication of Biomimetic Gecko Skin

Based upon studies found in literature, the dominant adhesive mechanism utilized by geckos and other spider attachment systems appears to be van der Waals forces. The complex divisions of the gecko skin (lamellae-setae-branches-spatulae) enable a large real area of contact between the gecko skin and mating surface. Hence, a hierarchical fibrillar micro/nanostructure is desirable for dry, super-adhesive tapes (Jagota and Bennison, 2002). The development of a nanocomposite capable of replicating this adhesive force developed in nature is limited by current fabrication techniques.

On the micro/nanoscale, typical machining methods (i.e. forging, drilling, grinding, lapping, etc.) are not possible. In order to create nanobumps, other manufacturing techniques are required and have been the subject of numerous studies (Geim et al., 2003; Sitti, 2003; Sitti and Fearing, 2003a, 2003b; Northen and Turner, 2005a, 2005b; Yurdumakan et al., 2005).

2.4.3.1 Single Level Hierarchical Structures

Previously, AFM tips have been used to create a set of dimples on a wax surface in a process like that of Figure 17. These dimples which served as a mold for creating polymer nanopyramids (Sitti and Fearing, 2003a). The adhesive force to an individual pyramid was measured using another AFM cantilever. The force was found to be about 200 μN. Although each pyramid of the material is capable of producing similar forces to that of a gecko seta, it failed to replicate adhesion on a large scale. This was due to the lack of flexibility in the pyramids. In order to ensure that the largest possible area of contact occurs between the tape and mating surface, a soft, compliant fibrillar structure

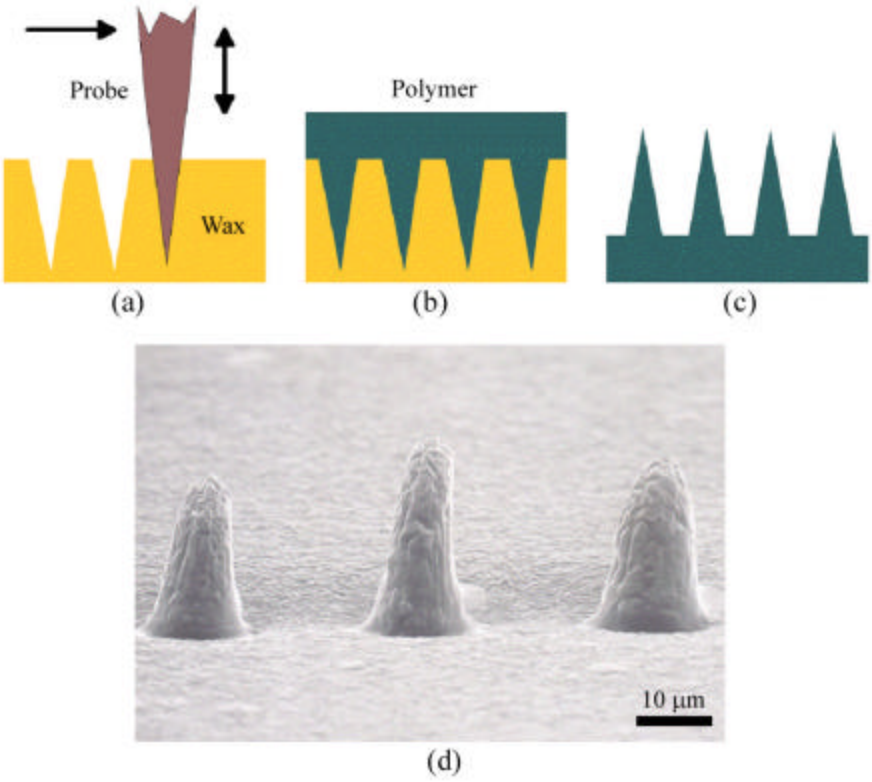

Fig. 17 (a) Indenting a flat wax surface using a sharp probe (nano-tip indenting), (b) molding with a polymer, and (c) separating the polymer from the wax surface by peeling. (d) SEM image of three pillars created by nano-tip indentation (Sitti, 2003).

would be desired (Jagota and Bennison, 2002). As shown in previous calculations, the van der Waals adhesive force is inversely proportional to the cube of the distance between two surfaces.

Geim et al. (2003) created arrays of nanohairs using electron-beam lithography and dry etching in oxygen plasma (Figure 18a). The original arrays were created on a rigid silicon wafer. This design was only capable of creating 0.01 N of adhesive force for a 1 cm^2 patch. The nanohairs were then transferred from the silicon wafer to a soft bonding substrate. A 1 cm^2 sample was able to create 3 N of adhesive force under the new arrangement. This is approximately one-third the adhesive strength of a gecko.

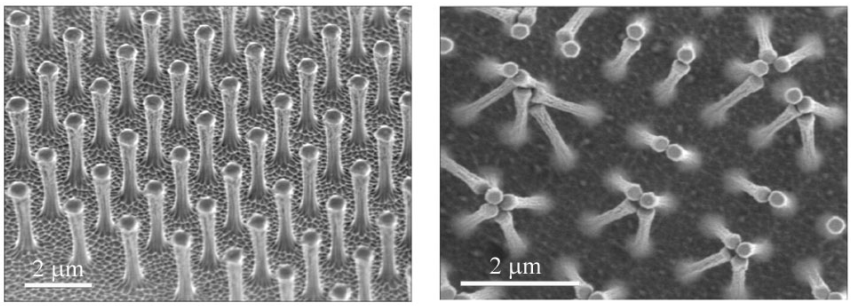

Fig. 18 SEM images of (a) an array of polyimide nanohairs and (b) bunching of the nanohairs, which leads to a reduction in adhesive force (Geim et al., 2003).

Bunching (as described earlier) was determined to greatly reduce the adhesive strength of the polymer tape. The bunching can be clearly seen in Figure 18b.

Multiwalled carbon nanotube (MWCNT) hairs have been used to create superadhesive tapes (Yurdumakan et al., 2005). The first step in the creation of this surface involves the growth of 50-100 μm MWCNT on quartz or silicon substrates through chemical vapor deposition. Patterns are then created using a combination of photolithography and a wet and/or dry etching. SEM images of the nanotube surfaces can be seen in Figure 19. On a small scale (nanometer level), the MWCNT surface was able to achieve adhesive forces 200 greater than those of gecko foot-hairs.

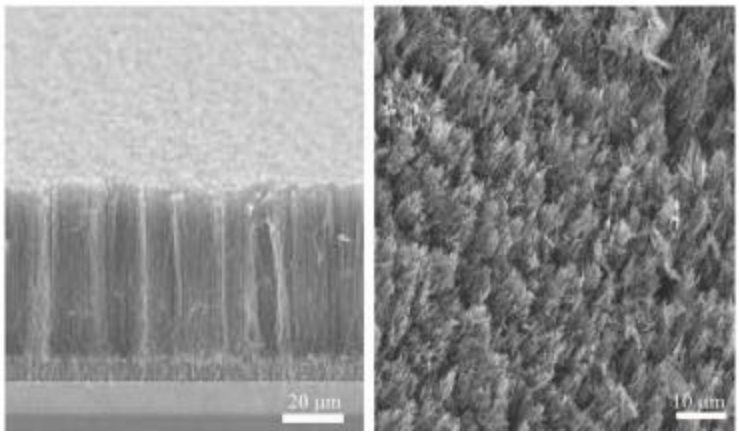

Fig. 19 SEM images of multi-walled carbon nanotube structures: (left) grown on silicon by vapor deposition, (right) transferred into a PMMA matrix and then exposed on the surface after solvent etching (Yurdumakan et al., 2005).

Directed self-assembly could be used to produce regularly spaced fibers (Schäffer et al. 2000; Sitti, 2003). In this technique, a thin liquid polymer film is coated on a flat conductive substrate. As demonstrated in Figure 20, a closely spaced metal plate is used to apply a DC electric field on the polymer film. Due to instabilities, pillars will begin to grow. Self-assembly is desirable because the components spontaneously assemble, typically by bouncing around in a solution or gas phase until a stable structure of minimum energy is reached. This method is crucial in biomolecular nanotechnology, and has the potential to be used in precise devices (Anonymous, 2002). These surface coatings have been demonstrated to be both durable and capable of creating superhydrophobic conditions and have been used to form clusters on the nanoscale (Pan et al., 2005).

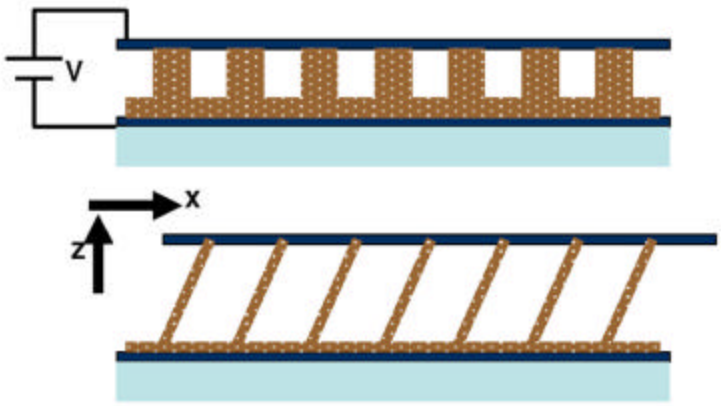

Fig. 20 Directed self-assembly based method of producing high aspect ratio micro/nanohairs (Sitti, 2003).

2.4.3.2 Multi-Level Hierarchical Structures

The aforementioned fabricated surfaces only have one level of hierarchy. Although these surfaces are capable of producing high adhesion on the micro/nanoscale, all have failed in producing large scale adhesion due to a lack of compliance and bunching. In order to overcome these problems, Northen and Turner (2005a, 2005b) created a multi-level compliant system by employing a microelectromechanical based approach. The created a layer of nanorods which they deemed "organorods" (Figure 21a). These organorods are comparable in size to that of gecko spatulae (50-200 nm in diameter and 2 μm tall). They sit atop silicon dioxide chip (approximately 2 μm thick and 100-150 μm across a side), which were created using photolithography (Figure 21b). Each chip is supported on top of a pillar (1 μm in diameter and 50 μm tall) that attaches to a silicon wafer (Figure 21c). The multilevel structures have been created across a 100 mm wafer (Figure 21d).

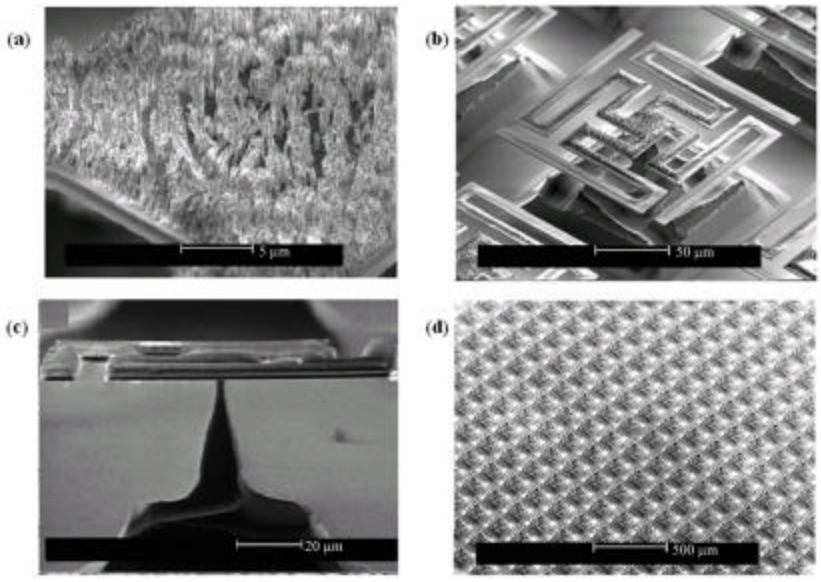

Fig. 21 Multilevel fabricated adhesive structure composed of (a) organorods, (b) silicon dioxide chips, and (c) support pillars. (d) This structure was repeated multiple times over a silicon wafer (Northen and Turner, 2005a, 2005b)

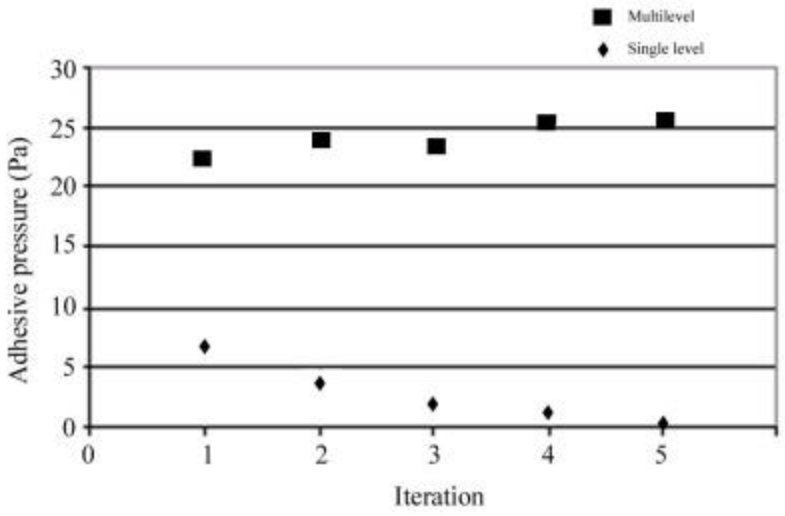

Fig. 22 Adhesion test results of a multilevel hierarchical structure (top) and a single level hierarchical structure (bottom) repeated for five iterations (Northen and Turner, 2005b).

Adhesion testing was performed using a nanorod surface on a solid substrate and on the multilevel structures. As seen in Figure 22, adhesive pressure of the multilevel structures was several times higher than that of the surfaces with only one level of hierarchy. The durability of the multilevel structure was also much greater than the single level structure. The adhesion of the multilevel structure did not change between iterations one and five. During the same number of iterations, the adhesive pressure of the single level structure decreased to zero.

Sitti (2003) proposed a nano-molding technique for creating structures with two levels of structures. In this method two different molds are created—one with pores on the order of magnitude of microns in diameter and a second with pores of nanometer scale diameter. As seen in Figure 23, the two molds would be bonded to each other and then filled with a liquid polymer. According to Sitti (2003), the method would enable the manufacturing of a high volume of synthetic gecko foot hairs at low cost.

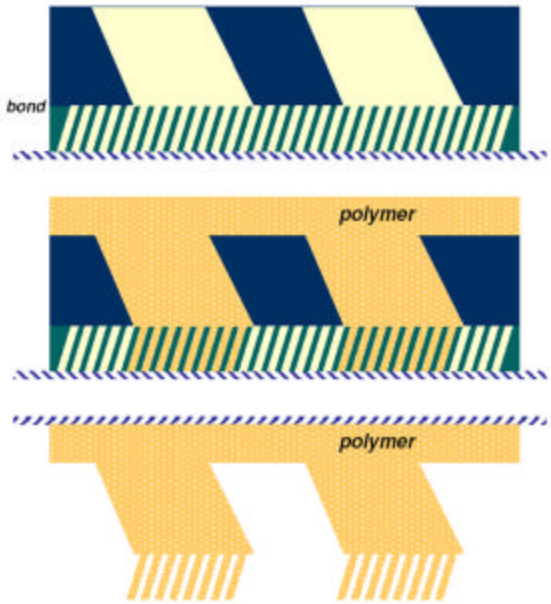

Fig. 23 Proposed process of creating multi-level synthetic gecko foot hairs using nano-molding. (a) Micron and nanometer sized pore membranes are bonded together and (b) filled with liquid polymer. (c) The membranes are then etched away leaving the polymer surface (Sitti, 2003).

Literature clearly indicates that in order to create a dry superadhesive, a fibrillar surface construction is necessary to maximize the van der Waals forces by decreasing the distance between the two surfaces. It is also desirable to have a superhydrophobic surface in order to utilize self cleaning. A material must be soft enough to conform to rough surfaces yet hard enough to avoid bunching, which will decrease the adhesive force.

Chapter 3

Surface Characterization, Adhesion, and Friction of a Bio-Inspired Reversible Adhesive Tape

A polyvinylsiloxane (PVS) sample that was fabricated with an array of closely packed micropillars was analyzed. The adhesion, friction force, surface construction, and contact angle of the structured sample were compared to that of an unstructured sample.

3.1 Experimental Details

3.1.1 Samples

For this study two samples—one with structured pillars and one unstructured—were characterized for surface roughness, contact angle, and friction force. The base of each sample is polyvinylsiloxane (PVS) (a two component dental wax), and the pillars of the structured sample are a nanocomposite. Adhesive force measurements using an atomic force microscope (AFM) (D3100, Nanoscope IIIa controller, Digital Instruments, Santa Barbara, CA) with a square pyramidal Si_3N_4 tip with a nominal radius of 30 nm on a triangular Si_3N_4 cantilever with a spring constant of 0.58 N/m and a 15 μm radius borosilicate ball mounted on a triangular Si_3N_4 cantilever with a spring constant of 0.58 N/m were unsuccessful in measuring the increased adhesion of the structured sample

because the effect of multiple pillars could not be measured with these small tips. For surface examination of the samples, scanning electron microscope (SEM) micrographs were taken with a JEOL JSM-820 Scanning Electron Microscope. The samples were affixed to aluminum stubs by double-sided conductive tape and air dried. All specimens were sputter-coated with less than 10 nm thick Au/Pd coating. The structured sample shown in Figure 24a, consists of an array of pillars of density about 230/mm^2 that are approximately 50 μm in diameter, 70 μm in height, and 60 μm center-to-center. The unstructured sample (Figure 24b) contains only random roughness.

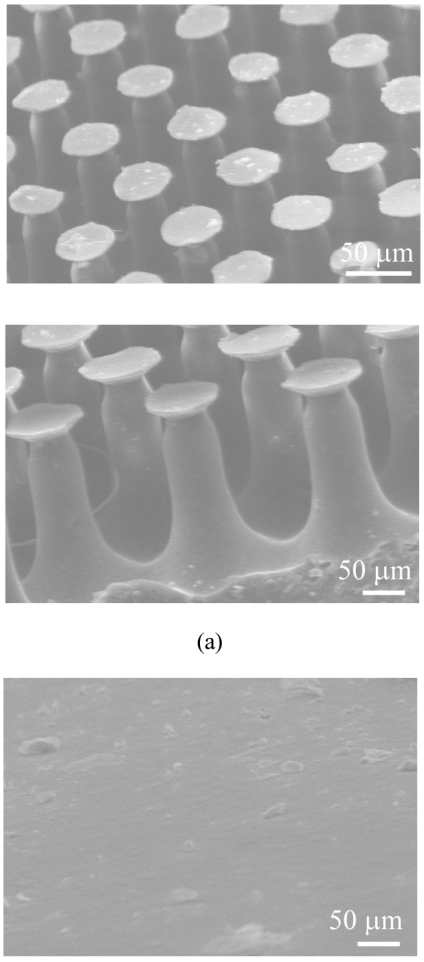

Fig. 24 SEM micrographs of (a) the pillars of the structured sample and (b) the unstructured sample.

3.1.2 Surface Roughness

The effect of micro/nanoscale surface roughness was determined by comparing the three-dimensional surface profile of the top of a single pillar on the structured sample to that of the unstructured sample. A commercial AFM (D3100, Nanoscope IIIa controller, Digital Instruments, Santa Barbara, CA) was used to obtain 2 μm x 2 μm and 10 μm x 10 μm scans. Originally, contact mode was used to obtain the scans. In contact mode, a square pyramidal Si_3N_4 tip with a nominal radius of 30 nm on a triangular Si_3N_4 cantilever with a spring constant of 0.58 N/m was used to measure surface roughness. Due to the compliance of the PVS samples, the tip would stick during scanning leading to poor surfaces images. To overcome this problem, tapping mode was used with a square pyramidal Si (100) tip with a native oxide layer which has a nominal radius of 20 nm on a rectangular Si (100) cantilever with a spring constant of 3 N/m. With this technique, more precise surface roughness was able to be measured.

The Z-range of the AFM used in the study is 7 μm. Since the pillars of the structured sample are much taller than the range of the AFM, an optical profiler (NT-3300, Wyko Corp., Tuscon, AZ) with a Z-range of 2 mm was used to determine the height of the pillars and obtain a 30 μm x 30 μm surface scan of both samples.

3.1.3 Friction

Nano/microscale friction measurements were not obtained of the surface because the effect of multiple pillars could not be measured with the technique. Macroscale frictional force was measured using a portable reciprocating friction tester (PREFT) in order to study the effects of multiple pillars on adhesion. For this test, the sample is

spliced in the middle of two pieces of tape. The test apparatus consists of a slide mounted on a base plate (Figure 3). A load cell is mounted on the slide, and one end of the tape is attached to the load cell. The other end of the tape is secured to a dead weight hanging freely. A variable speed DC motor is used to provide the reciprocating motion. The sample is then slid over a nominally flat glass slide. Before experimentation, the glass slide is cleaned with alcohol to remove any contamination.

The coefficient of friction, f, was then calculated (Bhushan, 1996)

$$f = \frac{1}{q} \ln\left(\frac{T_2}{T_1}\right) \tag{1}$$

where ? is the wrap angle, T_2 is the force during the pull of the PREFT, and T_1 is the force of the load.

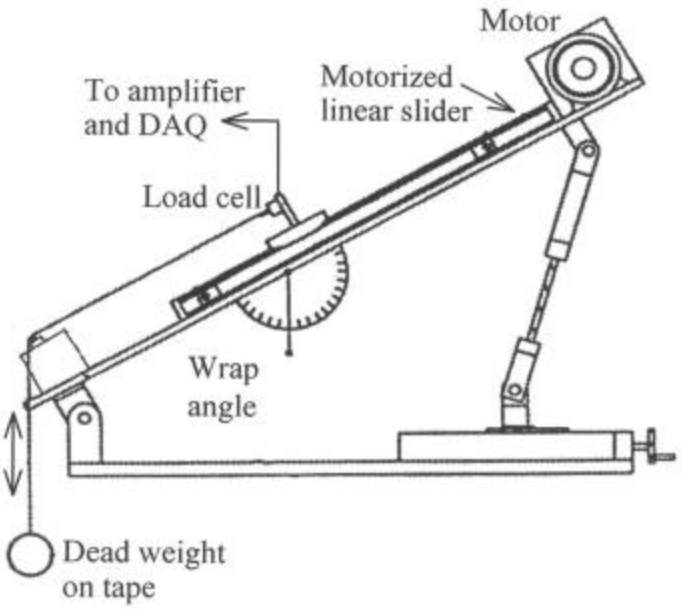

Fig. 25 Schematic of the portable reciprocating test apparatus for friction measurement (Bhushan, 1984).

3.1.4 Contact Angle

Contact angle, a measure of surface hydrophobicity, was measured for both samples using a NRL C.A. Model 100 Goniometer (Rame-Hart, Inc., Mountain Lakes, NJ). The measurements were made using demineralized, deionized water droplets. Surfaces that have a high contact angle with water exhibit self-cleaning properties called the "lotus effect" (Barthlott and Neinhius, 1997). Contact angle depends on a multitude of factors including the manner of surface preparation, surface cleanliness, and roughness (Adamson, 1990; Israelachvili, 1992; Bhushan, 1999, 2002, 2005; Burton and Bhushan, 2005; Bhushan and Jung, 2006). Wenzel (1936) developed an equation relating contact angle of a rough surface to the contact angle of a smooth surface of the same material

$$\cos q = R_f \cos q_o \qquad (2)$$

where ? is the contact angle of a rough surface, R_f is the roughness factor of the rough surface (ratio of total surface area of the rough surface to the projected area of the rough surface), and $?_o$ is the contact angle of a smooth surface. Since the roughness factor is always greater than or equal to one, Wenzel's equation predicts that introducing roughness to a hydrophilic surface (contact angle < 90º) will decrease the contact angle making the surface more hydrophilic, while introducing roughness to a hydrophobic surface (contact angle > 90º) will make the surface more hydrophobic.

3.2 Results and Discussion

The increased macroscale adhesive and frictional forces of the structured sample in comparison to the unstructured sample can be easily observed. If the structured sample is placed on a vertical surface, it will stick while the unstructured sample will fall off. When placed on a flat, horizontal surface and pulled parallel to the surface a large, constant frictional force arises with the structured sample. During sliding, broken contacts between the pillars and the sliding surface are constantly recreated, leading to high friction. During sliding of the unstructured sample, contact is permanently broken, resulting in smaller values of kinetic friction.

To investigate the effect of random roughness on adhesion, several surface parameters including roughness amplitude, R_q, the correlation length, ß*, peak to valley distance, P-V, and density of peaks, $?_p$ for both samples were studied for each scan size (2 µm x 2 µm, 10 µm x 10 µm, and 30 µm x 30 µm) (Bhushan, 2002, 2005). Three-dimensional and topographical surface profiles as well as a two-dimensional plot of the structured and unstructured samples are shown in Figure 4. As shown in Table 1, the only significant difference between the top of the pillars of the structured surface and the unstructured surface is the density of peaks at the scan sizes of 10 x 10 μm^2 and 2 x 2 μm^2 obtained with the AFM. The tops of the pillars of the structured sample have many more peaks than the unstructured sample. It is noteworthy that the density of peaks for the 10 µm scan size is about 2.3×10^7 which is on the same order of magnitude as the upper bound of the density of spatulae on a Tokay gecko (1.4×10^7).

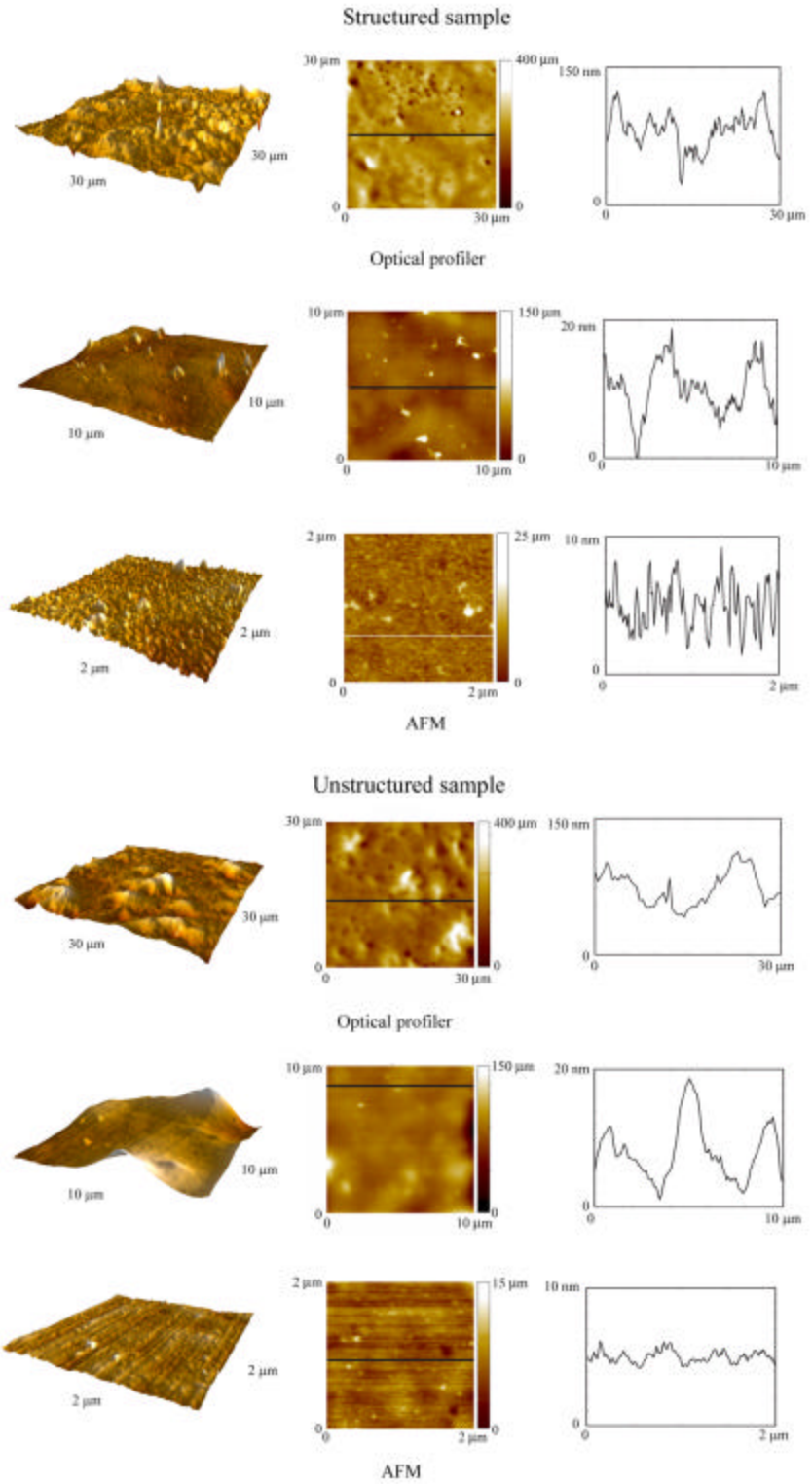

Fig. 26 Three-dimensional, topographical, and two-dimensional surface plots of (a) the top of a pillar of the structured sample and (b) the unstructured sample.

Table 1 – Surface roughness parameters for the top of a pillar of the structured sample and the unstructured sample at scan lengths of 30 µm, 10 µm, and 2 µm.

Measurement method	Scan size (µm)	Sample	R_q (nm)	ß* (µm)	P-V (nm)	$N_p/\mu m^2$
Optical profiler	30	Top of pillar	43	13	433	0.62
		Unstructured	36	6.3	451	0.68
AFM	10	Top of pillar	7.6	1.9	133	23
		Unstructured	8.7	4.5	86	1
	2	Top of pillar	2.2	0.1	26	654
		Unstructured	1.8	0.5	21	120

Based on the similarity in the analysis of the surface profiles of the top of the pillars of the structured sample and the unstructured sample, it can be concluded that the increased adhesive and frictional force of the structured sample is a result of the structured roughness of the sample. Random roughness does not is not the cause of high adhesion.

The frictional and adhesive force enhancement created by bio-inspired surfaces is due to the division of contacts—structured roughness—of the surface. Since the structured and unstructured samples are both made of PVS it is expected that adhesion and friction enhancement would not occur on the nano/microscale, but these effects would be observed on the macroscale when multiple pillars of the structured sample are in contact with a surface at the same time. Testing with the PREFT yielded a 39% increase in the coefficient of friction from the unstructured sample (0.27) and the structured sample (0.37) (Figure 5). The results of the friction and adhesion testing leads to the conclusion that structured roughness is important in adhesion enhancement while random roughness has little effect.

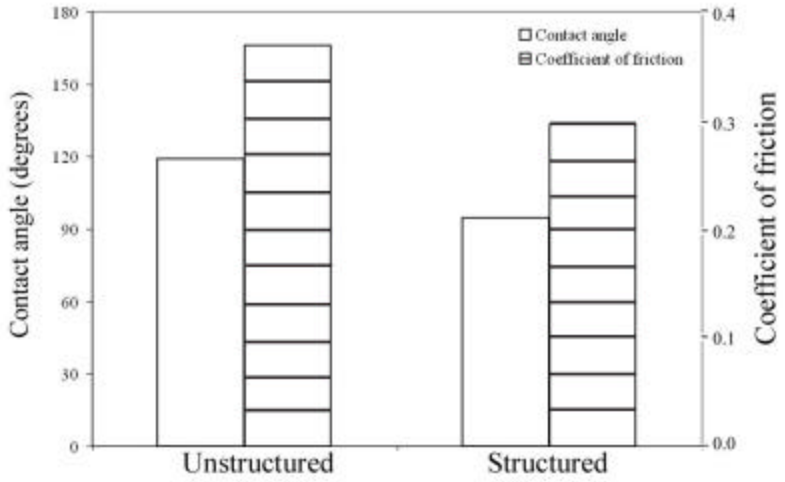

Fig. 5 Contact angle and coefficient of friction of against glass with a normal load of 130 mN of the structured and unstructured samples.

The contact angle of the unstructured sample is 94.5º ± 0.5º. Due to the increased roughness of the structured sample from the pillars, the contact angle increased roughly 40º to 133.3º ± 2.5º. These results, depicted in Figure 5, show that not only does dividing a surface into smaller contacts increase friction and adhesion; it also leads to self cleaning by increased contact angle. Self cleaning enables the adhesive to be used multiple times without dirt particles contaminating the surface

Chapter 4

Closure

The adhesive properties of geckos and other creatures such as flies, beetles and spiders, are due to the hierarchical structures present on each creature's attachment pads. Geckos have developed the most intricate adhesive structures of any of the aforementioned creatures. The attachment system consists of ridges called lamellae that are covered in microscale setae that branch off into nanoscale spatulae. Each structure plays an important role in adapting to surface roughness bringing the spatulae in close proximity with the mating surface. These structures as well as material properties allow the gecko to obtain a much larger real area of contact between its feet and a mating surface than is possible with a non-fibrillar material. Two feet of a Tokay gecko have about 220 mm^2 of attachment pad area on with which the gecko is able to generate approximately 20 N of adhesive force. Although capable of generating high adhesive forces, a gecko is able to detach from a surface at will—an ability known as smart adhesion. Detachment is achieved by a peeling motion of the gecko's feet from a surface.

van der Waals forces are widely accepted in literature as the dominant adhesive mechanism utilized by hierarchical attachment systems. Capillary forces created by humidity naturally present in the air can further increase the adhesive force generated by the spatulae. Experimental results have supported the adhesive theories of intermolecular forces (van der Waals) as a primary adhesive mechanism and capillary forces as a secondary mechanism, and have been used to rule out several other mechanisms of adhesion including the secretion of sticky fluids, suction, and increased frictional forces. Atomic force microscopy has been employed by several investigators to determine the adhesive strength of gecko foot hairs. The measured values of the maximum adhesive force of a single seta (194 μN) and of a single spatula (11 nN) are comparable to the van der Waals prediction of 270 μN and 11nN for a seta and spatula, respectively. The adhesive force generated by seta increases with preload and reaches a maximum when both perpendicular and parallel preloads are applied. Although gecko feet are strong adhesives, they remain free of contaminant particles through self cleaning. Spatular size along with material properties enable geckos to easily expel any dust particles that come into contact with their feet.

There is a great interest among the scientific community to create surfaces that replicate the adhesive strength of gecko feet. These surfaces would be capable of reusable dry adhesion and would have uses in a wide range of applications from everyday objects such as tape, fasteners, and toys to microelectric and space applications and even wall-climbing robots. In the design of fibrillar structures, it is necessary to ensure that the fibrils are compliant enough to easily deform to the mating surface's roughness profile, yet rigid enough to not collapse under their own weight. Spacing of the

individual fibrils is also important. If the spacing is too small, adjacent fibrils can attract each other through intermolecular forces which will lead to bunching.

Nano-indentation, electron-beam lithography, and growing of carbon nanotube arrays are all methods that have been used to create fibrillar structures. The limitations of current machining methods on the micro/nanoscale have resulted in the majority of fabricated surfaces consisting of only one level of hierarchy. Although typically capable of producing high adhesive force with an individual fibril, all of these surfaces have failed to generate high adhesive forces on the macroscale. Bunching, lack of compliance, and lack of durability are all problems that have arisen with the aforementioned structures. Recently, a multi-layered compliant system was created using a microelectromechanical based approach in combination with nanorods. This method as well as other proposed methods of multilevel nano-molding and directed self assembly show great promise in the creation of adhesive structures with multiple levels of hierarchy, much like those of gecko feet.

Adhesion and friction enhancement in bio-inspired reversible adhesive tapes occurs due to structured roughness. Random roughness does not play a role in the high adhesive and friction forces created by these materials. Increased roughness on the structured surfaces also increases the contact angle of the surface which leads to self cleaning.

References

Adamson, A.V. (1990) *Physical Chemistry of Surfaces*, Wiley, NY.

Anonymous (2002), "Self-assembly," *Merriam-Webster's Medical Dictionary*, Merriam-Webster.

Aristotle, *Historia Animalium*, trans. Thompson, D.A.W. (1918), <http://classics.mit.edu/Aristotle/history_anim.html>.

Arzt, E., Gorb, S. and Spolenak, R. (2003), "From micro to nano contacts in biological attachment devices," *Proc. Natl. Acad. Sci.* **100**, 10603-10606.

Autumn, K. (2006), "How Gecko Toes Stick," *Am. Scientist*, **94**, 124-132.

Autumn, K. and Peattie, A.M. (2002), "Mechanisms of adhesion in geckos," *Integr. Comp. Biol.* **42**, 1081-1090.

Autumn, K., Liang, Y.A., Hsieh, S.T., Zesch, W., Chan, W.P., Kenny, T.W., Fearing, R. and Full., R.J. (2000), "Adhesive force of a single gecko foot-hair." *Nature*, **405**, 681-685.

Autumn, K., Sitti, M., Liang, Y.A., Peattie, A.M., Hansen, W.R., Sponberg, S., Kenny, T.W., Fearing, R., Israelachvili, J.N. and Full R.J. (2002), "Evidence for van der Waals adhesion in gecko setae," *Proc. Natl. Acad. Sci.* **99**, 12252-12256.

Barthlott, W. and Neinhuis, C. (1997), "Purity of the sacred lotus, or escape from contamination in biological surfaces," *Planta* **202**, 1-8.

Bergmann, P.J. and Irschick, D.J. (2005), "Effects of temperature on maximum clinging ability in a diurnal gecko: evidence for a passive clinging mechanism?" *J. Exp. Zool.* **303A**, 785-791.

Bertram, J. E. A. and Gosline, J. M. (1987), "Functional design of horse hoof keratin: the modulation of mechanical properties through hydration effects", *J. Exp. Biol.* **130**, 121-136.

Bhushan, B. (1984), "Influence of test parameters on the measurement of the coefficient of friction of magnetic tapes," *Wear* **93**, 81-99.

Bhushan, B. (1996), *Tribology and Mechanics of Magnetic Storage Devices*, 2nd Ed., Springer-Verlag, New York.

Bhushan, B. (1999), *Handbook of Micro/Nanotribology*, 2nd ed., CRC Press, Boca Raton, FL.

Bhushan, B. (1999), *Principles and Applications of Tribology*, Wiley, New York.

Bhushan, B. (2002), *Introduction to Tribology*, Wiley, New York.

Bhushan, B. (2003), "Adhesion and stiction: mechanisms, measurement techniques and methods for reduction," *J. Vac. Sci. Technol B.* **21**, 2262-2296.

Bhushan, B. (2005), *Introduction to Nanotribology and Nanomechanics*, Springer-Verlag, Heidelberg, Germany.

Bhushan, B. (2006), *Springer Handbook of Nanotechnology*, 2nd Ed., Springer-Verlag, Heidelberg, Germany.

Bhushan, B. and Jung, Y. C. (2006), "Micro- and Nanoscale Characterization of Hydrophobic and Hydrophilic Leaf Surfaces," *Nanotechnology* (in press).

Bhushan, B., Peressadko, A.G., and Kim, T.W. (2006) "Adhesion analysis of two-level hierarchical morphology in natural attachment systems for smart adhesion," submitted for publication.

Bikerman, J.J. (1961), *The Science of Adhesive Joints*, Academic, New York.

Burton, Z. and Bhushan, B. (2005), "Hydrophobicity, adhesion, and friction properties of nanopatterned polymers and scale dependence for micro- and nanoelectromechanical systems," *Nano Letters* **5**, 1607-1613.

Chui, B.W., Kenny, T.W., Mamin, H.J., Terris, B.D. and Rugar, D. (1998), "Independent detection of vertical and lateral forces with a sidewall-implanted dual-axis piezoresistive cantilever," *Appl. Phys. Lett.* **72**, 1388-1390.

Davies, D.K. (1973), "Surface charge and the contact of elastic solids," *J. Phys. D: Appl. Phys.* 6, 1017-1024.

Dellit, W.D. (1934), "Zur anatomie und physiologie der Geckozehe," *Jena. Z. Naturw.*, **68**, 613-658.

Derjaguin, B.V., Krotova, N.A. and Smilga, V.P. (1978), "Effect of contact deformations on the adhesion of particles," *J. Colloid Interface Sci.* **53**, 314-326.

Fan, P.L. and O'Brien, M.J. (1975), "Adhesion in deformable isolated capillaries," *Adhesion Science and Technology*, ed. Lee, L.H., **9A**, 635, Plenum, New York.

Federle, W., Riehle, M., Curtis, A.S.G. and Full, R.J. (2002), "An integrative study of insect adhesion: mechanics of wet adhesion of pretarsal pads in ants," *Integr. Comp. Biol.* **42**, 1100-1106.

Full, R.J., Fearing, R.S., Kenny, T.W. and Autumn, K. (2004), "Adhesive microstructure and method of forming same," *US Patent #6737160.*

Gao, H., Wang, X., Yao, H., Gorb, S. and Arzt, E. (2005), "Mechanics of hierarchical adhesion structures of geckos," *Mech. Mater.* **37**, 275-285.

Geim, A.K., Dubonos, S.V., Grigorieva, I.V., Novoselov, K.S., Zhukov, A.A. and Shapoval, S.Y. (2003), "Microfabricated adhesive mimicking gecko foot-hair," *Nat. Mater.* **2**, 461-463.

Gennaro, J.G.J. (1969), "The gecko grip," *Nat. Hist.* **78**, 36-43.

Glassmaker, N.J., Jagota, A., Hui, C.Y. and Kim, J. (2004), "Design of biomimetic fibrillar interfaces: 1. Making contact," *J. R. Soc. Interface* **1**, 23-33.

Glassmaker, N.J., Jagota, A. and Hui, C.Y. (2005), "Adhesion enhancement in a biomimetic fibrillar interface," *Acta Biomaterialia* **1**, 367-375.

Hamaker, H.C. (1937), "London van der Waals attraction between spherical bodies," *Physica*, **4**, 1058.

Hanna, G. and Barnes, W.J.P. (1991), "Adhesion and detachment of the toe pads of tree frogs," *J. Exper. Biol.* **155**, 103-125.

Hansen, W.R. and Autumn, K. (2005), "Evidence for self-cleaning in gecko setae," *Proc. Natl. Acad. Sci.* **102**, 385-389.

Henry, P.S.H. (1953), "The role of asymmetric rubbing in the generation of static electricity," *Brit. J. Appl. Phys.* **S2**, S31-S36.

Hiller, U. (1968), "Untersuchungen zum Feinbau und zur Funktion der Haftborsten von Reptilien," *Z. Morphol. Tiere,* **62**, 307-362.

Hinds, W.C. (1982), *Aerosol Technology: Properties, Behavior, and Measurement of Airborne Particles,* Wiley, New York.

Hora, S.L. (1923), "The adhesive apparatus on the toes of certain geckos and tree frogs," *J. Proc. Asiat. Soc. Beng.* **9**, 137-145.

Houwink, R. and Salomon, G. (1967), "Effect of contamination on the adhesion of metallic couples in ultra high vacuum," *J. Appl. Phys.* **38**, 1896-1904.

Huber, G., Gorb, S.N., Spolenak, R. and Arzt, E. (2005a), "Resolving the nanoscale adhesion of individual gecko spatulae by atomic force microscopy." *Biol. Lett.* **1**, 2-4.

Huber, G., Mantz, H., Spolenak, R., Mecke, K., Jacobs, K., Gorb, S.N. and Arzt, E. (2005b), "Evidence for capillarity contributions to gecko adhesion from single spatula and nanomechanical measurements," *Proc. Natl. Acad. Sci.* **102**, 16293-16296.

Hui, C.Y., Jagota, A., Lin, Y.Y. and Kramer, E.J. (2002), "Constraints on micro-contact printing imposed by stamp deformation," *Langmuir*, **18**, 1394-1404.

Irschick, D.J., Austin, C.C., Petren, K., Fisher, R.N., Losos, J.B. and Ellers, O. (1996), "A comparative analysis of clinging ability among pad-bearing lizards," *Biol. J. Linn. Soc.* **59**, 21-35.

Israelachvili, J.N. and Tabor, D. (1972), "The measurement of Van der Waals dispersion forces in the range of 1.5 to 130 nm," *Proc. R. Soc. Lond. A.* **331**, 19-38.

Israelachvili, J.N. (1992), *Intermolecular and Surface Forces*, 2nd edition, Academic, San Diego.

Jaenicke, R. (1998) "Atmospheric aerosol size distribution," *Atmospheric Particles*, Ed. Harrison, R.M. and van Grieken, R., Wiley, New York, 1-29.

Jagota, A. and Bennison, S.J. (2002), "Mechanics of adhesion through a fibrillar microstructure," *Integr. Comp. Biol.* **42**, 1140-1145.

Johnsen, A. and Rahbek, K. (1923), "A pysical phenomenon and its applications to telegraphy, telephony, etc.," *J. Instn. Elec. Engrs.* **61**, 713-725.

Johnson, K.L., Kendall, K. and Roberts, A.D. (1971), "Surface energy and the contact of elastic solids," *Proc. R. Soc. Lond. A.* **324**, 301-313.

Losos, J.B. (1990), "Thermal sensitivity of sprinting and clinging performance in the tokay gecko (*Gekko gecko)*," *Asiat. Herp. Res.* **3**, 54-59.

McFarlane, J.S. and Tabor, D. (1950), "Adhesion of solids and the effects of surface films," *Proc. R. Soc. Lond. A.* **202**, 224-243.

Menon, C., Murphy, M. and Sitti, M. (2004) "Gecko inspired surface climbing robots," *IEEE Int. Conf. on Robotics and Biomimetics*, August 22-26, 431-436.

Northen, M.T. and Turner, K.L. (2005a), "A batch fabricated biomimetic dry adhesive," *Nanotechnology*, **16**, 1159-1166.

Northen, M.T. and Turner, K.L. (2005b), "Multi-scale compliant structures for use as a chip scale dry adhesive," *Transducers*, **2**, 2044-2047.

Pan, B., Gao, F., Ao, L., Tian, H., He, R. and Cui, D. (2005), "Controlled self-assembly of thiol-terminated poly(amidoamine) dendrimer and gold nanoparticles," *Colloids and Surfaces A*, **259**, 89-94.

Peressadko, A. and Gorb, S.N. (2004), "When less is more: experimental evidence for tenacity enhancement by division of contact area," *J. Adhesion*, **80**, 247-261.

Persson, B.N.J. (2003), "On the mechanism of adhesion in biological systems," *J. Chem. Phys.* **118**, 7614-7621.

Persson, B.N.J. and Gorb, S. (2003), "The effect of surface roughness on the adhesion of elastic plates with application to biological systems," *J. Chem. Phys.* **119**, 11437-11444.

Phipps, P.B. and Rice, D.W. (1979), "Role of water in atmospheric corrosion," *ACS Symposium Series No. 89.*

Ruibal, R. and Ernst, V. (1965), "The structure of the digital setae of lizards," *J. Morph.* **117**, 271-294.

Russell, A.P. (1975), "A contribution to the functional morphology of the foot of the tokay, *Gekko gecko*," *J. Zool. Lond.* **176**, 437-476.

Russell, A.P. (1986), "The morphological basis of weight-bearing in the scansors of the tokay gecko," *Can. J. Zool.* **64**, 948-955.

Schäffer, E., Thurn-Albrecht, T., Russell, T.P. and Steiner, U. (2000) "Electrically induced structure formation and pattern transfer," *Nature*, **403**, 874-877.

Schleich, H.H. and Kästle, W. (1986), "Ultrastrukturen an Gecko-Zehen," *Amphibia Reptilia*, **7**, 141-166.

Schmidt, H.R. (1904), "Zur Anatomie und Physiologie der Geckopfote," *Jena. Z. Naturw.* **39**, 551.

Shah, G.J. and Sitti, M. (2004), "Modeling and design of biomimetic adhesives inspired by gecko foot-hairs," *IEEE Int. Conf. on Robotics and Biomimetics*, August 22-26, 873-878.

Shaw, P.E. (1923), "Electrical separation between identical solid surfaces," Proc. Phys. Soc. **39**, 449-452.

Simmermacher, G. (1884), "Untersuchungen uber haftapparate an tarsalgliedern von insekten," *Zeitschr. Wiss. Zool.* **40**, 481-556.

Sitti, M. (2003) "High aspect ratio polymer micro/nano-structure manufacturing using nanoembossing, nanomolding and directed self-assembly," *Proc. IEEE/ASME Advanced Mechatronics Conf*. July 20-24, 2, 886-890.

Sitti, M. and Fearing, R.S. (2002) "Nanomodeling based fabrication of synthetic gecko foot-hairs," *Proc. IEEE Conf. Nanotechnology,* August 26-28, 137-140.

Sitti, M. and Fearing, R.S. (2003a) "Synthetic gecko foot-hair for micro/nano structures as dry adhesives," *J. Adhesion Sci. Technol.* **18**, 1055-1074.

Sitti, M. and Fearing, R.S. (2003b) "Synthetic gecko foot-hair for micro/nano structures for future wall-climbing robots," *Proc. IEEE Int. Conf. on Robotics and Automation*, September 14-19, **1**, 1164-1170.

Skinner, S.M., Savage, R.L. and Rutzler, J.E. (1953), "Electrical phenomena in adhesion I: electron atmospheres in dielectrics," *J. App. Phys.* **24**, 438-450.

Stork, N.E. (1980), "Experimental analysis of adhesion of *Chrysolina polita* on a variety of surfaces," *J. Exp. Biol.* **88**, 91-107.

Stork, N.E. (1983), *J. Nat. Hist*., **17**, 829-835.

Timoshenko, S.P. and Gere, J.M. (1961), *Theory of elastic stability*, McGraw-Hill.

Tinkle, D.W. (1992), "Gecko," *Encylcopedia Americana*, Grolier, **12**, 359.

Van der Kloot, W.G. (1992), "Molting," *Encylcopedia Americana*, Grolier, **19**, 336-337.

Wagler, J. (1830), *Naturliches System der Amphibien*, J. G. Cotta'schen Buchhandlung, Munich.

Wahlin, A. and Backstrom, G. (1974), "Sliding electrification of teflon by metals," *J. Appl. Phys.* **45**, 2058-2064.

Wenzel, R. N. (1936), "Resistance of solid surfaces to wetting by water," *Indust. Eng. Chem.* **28**, 988-994.

Williams, E.E. and Peterson, J.A. (1982), "Convergent and alternative designs in the digital adhesive pads of scincid lizards," *Science* **215**, 1509-1511.

Yurdumakan, B., Raravikar, N.R., Ajayan, P.M. and Dhinojwala, A. (2005), "Synthetic gecko foot-hairs from multiwalled carbon nanotubes," *Chem. Comm.* 3799-3801.

Zimon, A.D. (1969), *Adhesion of Dust and Powder*, translated from Russian by M. Corn, Plenum, New York.

Zisman, W.A. (1963), “Influence of constitution on adhesion,” *Ind. Eng. Chem.* **55** (10), 18-38.

Appendix A

Typical Rough Surfaces

Several natural (sycamore tree bark and siltstone) and artificial surfaces (dry wall, wood laminate, steel, aluminum, and glass) were chosen to determine the microscale surface parameters of typical rough surfaces that a gecko might encounter. An Alpha-step® 200 (Tencor Instruments, Mountain View, CA) was used to obtain surface profiles three different length scales, 80 µm, which is approximately the size of a single gecko seta, 2000 µm, which is close to the size of a gecko lamella, and an intermediate scan length of 400 µm. The radius of the stylus tip was 1.5-2.5 µm and the applied normal load was 3 mg. The surface profiles were then analyzed using a specialized computer program to determine the root mean square amplitude, s, correlation length, ß*, peak to valley distance, P-V, skewness, Sk, and kurtosis, K.

Samples of surface profiles and their corresponding parameters at a scan length of 2000 µm can be seen in Figure A.1a. The roughness amplitude, s, varies from as low as 0.01 µm in glass to as high as 30 µm in tree bark. Similarly, correlation length varies

Table A.1 Scale dependence of surface parameters s and ß* for rough surfaces at scan lengths of 80 µm and 2000 µm.

Scan length	**80 µm**		2000 µm	
surface	s **(µm)**	b^* **(µm)**	s **(µm)**	b^* **(µm)**
Sycamore tree bark	4.4	17	27	251
Silitstone	1.1	4.8	11	268
Painted drywall	1	11	20	93
Wood laminate	0.11	18	3.6	264
Polished steel	0.07	12	0.40	304
Polished 2024 aluminum	0.40	6.5	0.50	222
Glass	0.01	2.2	0.02	152

from 2-300 µm. The scale dependency of surface parameters is illustrated in Figure A.1b. As the scan length of the profile increases, so to does the roughness amplitude and correlation length. Table A.1 summarizes the scale dependent factors s and ß* for all seven sampled surfaces. At a scale length of 80 µm (size of seta), the roughness amplitude does not exceed 5 µm while at a scale length of 2000 µm (size of lamella), the roughness amplitude is as high as 30µm. This suggests that setae are responsible to adapt to surfaces with roughness on the order of several microns while lamellae must adapt to roughness on the order of tens of microns. Greater roughness values would be adapted to by the skin of the gecko. The spring model of Bhushan et al. (2006) verifies that setae are only capable of adapting to roughness of a few microns and suggests that lamellae are responsible for adaptation to rougher surfaces.

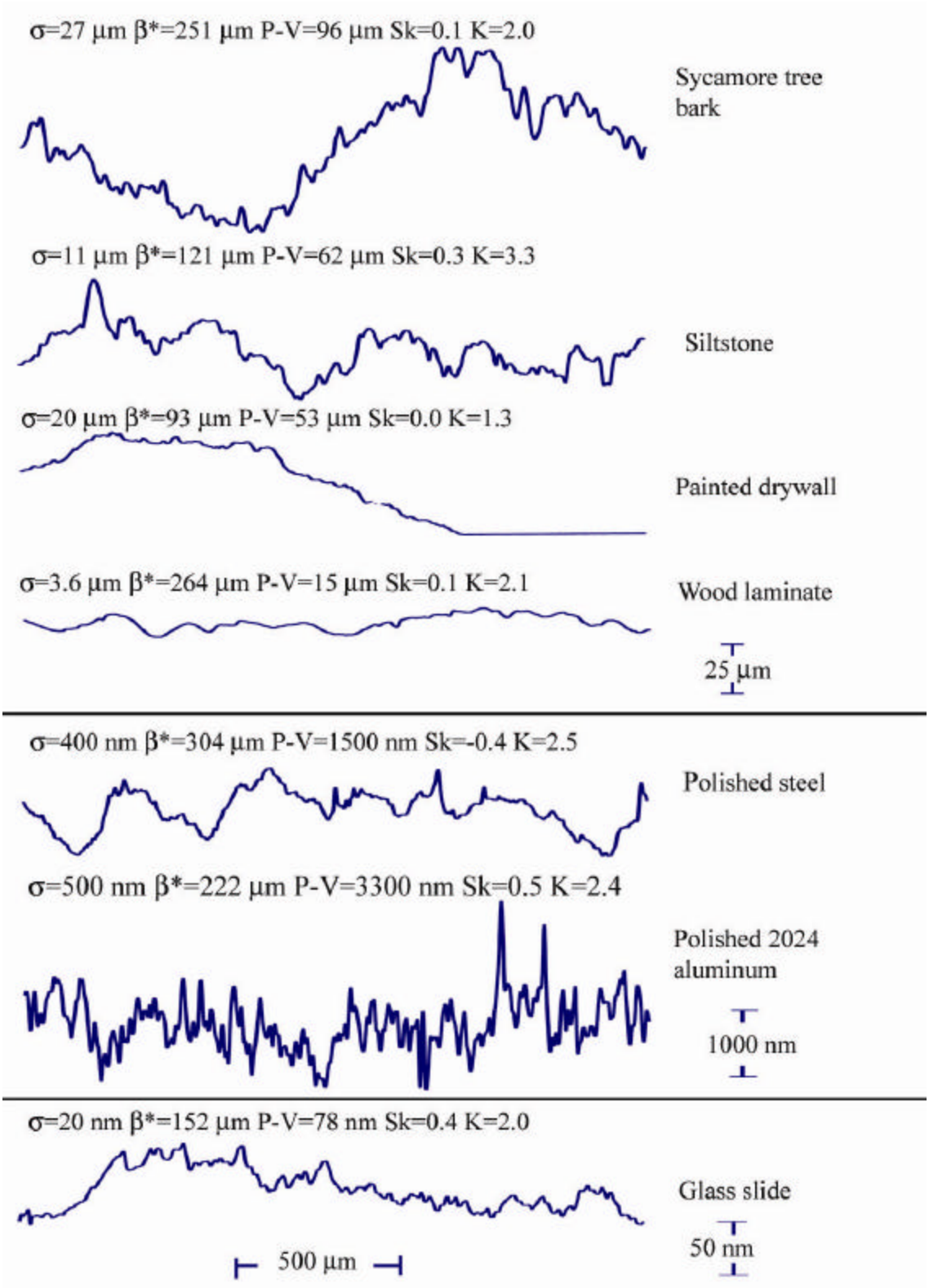

Fig. A.1 (a) Surface height profiles of various random rough surfaces of interest at a 2000 μm scan length.

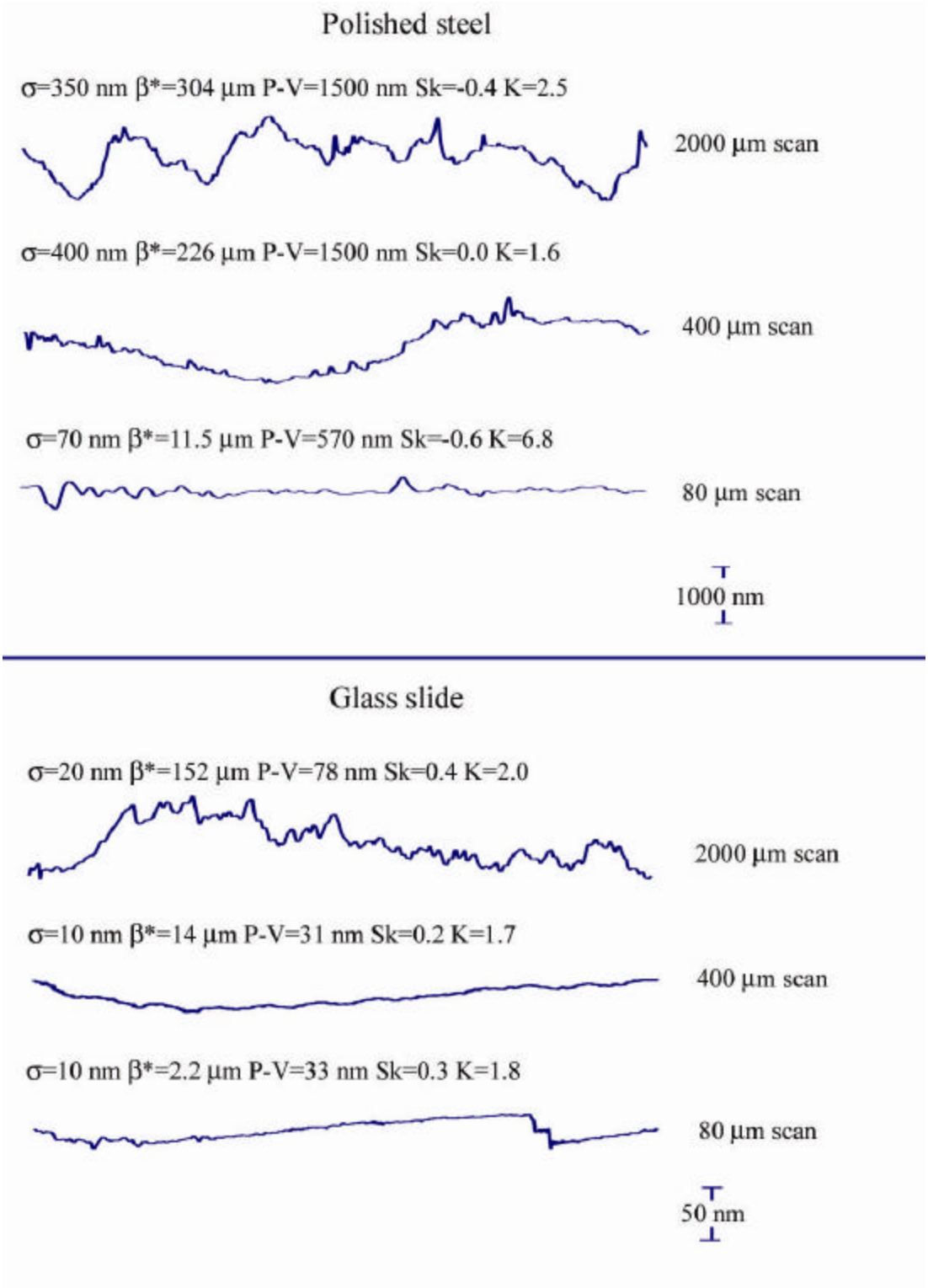

Fig. A.1 (b) A comparison of the profiles of two surfaces at 80, 400, and 2000 µm scan lengths.